Role of Three Rab5-like GTPases, Ypt51p, Ypt52p, and Ypt53p, in the Endocytic and Vacuolar Protein Sorting Pathways of Yeast

Birgit Singer-Krüger,* Harald Stenmark,* Andreas Düsterhöft,‡ Peter Philippsen,‡ Jin-San Yoo,§ Dieter Gallwitz,§ and Marino Zerial*

*EMBL, Postfach 10.22.09, D-69012 Heidelberg, Germany; ‡Institut für Mikrobiologie u. Molekularbiologie, Universität Giessen, D-6300 Giessen, Germany; and §Max-Planck-Institut für Biophysikalische Chemie, Abteilung Molekulare Genetik, Postfach 28.41, D-37018 Göttingen, Germany

Abstract. The small GTPase rab5 has been shown to represent a key regulator in the endocytic pathway of mammalian cells. Using a PCR approach to identify rab5 homologs in *Saccharomyces cerevisiae*, two genes encoding proteins with 54 and 52% identity to rab5, *YPT51* and *YPT53* have been identified. Sequencing of the yeast chromosome XI has revealed a third rab5-like gene, *YPT52*, whose protein product exhibits a similar identity to rab5 and the other two *YPT* gene products. In addition to the high degree of identity/homology shared between rab5 and Ypt51p, Ypt52p, and Ypt53p, evidence for functional homology between the mammalian and yeast proteins is provided by phenotypic characterization of single, double, and triple deletion mutants. Endocytic delivery to the vacuole of two markers, lucifer yellow CH (LY) and α-factor, was inhibited in *Δypt51* mutants and aggravated in the double *ypt51ypt52* and triple *ypt51ypt52ypt53* mutants, suggesting a requirement for these small GTPases in endocytic membrane traffic. In addition to these defects, the here described *ypt* mutants displayed a number of other phenotypes reminiscent of some vacuolar protein sorting (*vps*) mutants, including a differential delay in growth and vacuolar protein maturation, partial missorting of a soluble vacuolar hydrolase, and alterations in vacuole acidification and morphology. In fact, *vps21* represents a mutant allele of *YPT51* (Emr, S., personal communication). Altogether, these data suggest that Ypt51p, Ypt52p, and Ypt53p are required for transport in the endocytic pathway and for correct sorting of vacuolar hydrolases suggesting a possible intersection of the endocytic with the vacuolar sorting pathway.

In eukaryotic cells endocytosis is a basic process by which extracellular molecules are internalized by invaginating and pinching off parts of the plasma membrane. This membrane transport pathway has been extensively studied also in the budding yeast *Saccharomyces cerevisiae* using two endocytic markers, Lucifer yellow CH (LY)[1] to follow fluid-phase endocytosis and α-factor to follow receptor-mediated endocytosis (for review see Riezman, 1993).

The availability of a large pool of mutants and the ease of isolation of novel ones has made the budding yeast *S. cerevisiae* an excellent system to study the in vivo functions of proteins in the process of endocytosis and to identify novel components of the endocytic machinery. For example, the requirement for clathrin heavy chain (Payne et al., 1988), actin and the actin-binding protein Sac6p (Kübler and Riezman, 1993) in the step of endocytic internalization has been recently established by such analysis. Genetic screens for mutants defective in the internalization of endocytic markers and their delivery to the vacuole have furthermore resulted in the identification of End3p and End4p (Raths et al., 1993) and Renlp/Vps2p (Davis et al., 1993), whose precise functions in endocytic membrane traffic are however yet unknown.

Another class of proteins that is believed to be required for endocytic transport is the family of small GTPases, known as Ypt family in yeast and rab family in mammalian cells. Their key regulatory role in intracellular membrane traffic was initially demonstrated with the help of conditional lethal yeast mutants, *sec4* and *ypt1*, in the secretory pathway (Salminen and Novick, 1987; Segev et al., 1988; Schmitt et al., 1988). In mammalian cells a large number of proteins belonging to the rab family have been identified due to their similarity in primary structure to Ypt1p and Sec4p (Haubruck et al., 1987; Touchot et al., 1987; Zahraoui et al.,

Address all correspondence to M. Zerial, EMBL, Meyerhofstrasse 1, Postfach 10.22.09, D-69012 Heidelberg, Germany.

1. *Abbreviations used in this paper:* ALP, alkaline phosphatase; CPY, carboxypeptidase Y; FR, flanking region; LY, Lucifer yellow.

1989; Chavrier et al., 1990). Some of these GTPases have been localized to distinct subcellular compartments of both the exocytic and endocytic pathways (for review see Zerial and Stenmark, 1993).

Members of the rab family that are specifically associated with elements of the endocytic apparatus are rab4, rab5, rab7, and rab9. Whereas rab4 and rab5 are located on early endosomes (Chavrier et al., 1990; van der Sluijs et al., 1991) and have a regulatory function in early steps of endocytosis (Bucci et al., 1992; van der Sluijs et al., 1992), rab7 and rab9 are associated with late endosomes and therefore are involved in later steps of the pathway (Chavrier et al., 1990; Lombardi et al., 1993). In *S. cerevisiae* a homolog of rab7, Ypt7p, has recently been identified (Wichmann et al., 1992). The *ypt7* null mutant is characterized by a delay of endocytic delivery of α-factor to the vacuole and by defects of vacuolar protein sorting and maturation (Wichmann et al., 1992).

In contrast to the proposed involvement of rab7 and Ypt7p in later steps of endocytosis, studies on rab5 have suggested a key regulatory role of this small GTPase in early endocytic traffic. Rab5 was found to be required for the fusion of early endosomes in vitro (Gorvel et al., 1991). In vivo, overexpression of the wild-type protein in BHK cells led to increased internalization of endocytic markers and to the appearance of very large early endosomal structures (Bucci et al., 1992). Conversely, expression of a mutant form of rab5, rab5Ile^{133}, inhibited endocytosis and resulted in fragmentation of early endosomes.

In the fission yeast *Schizosaccharomyces pombe* a homolog of rab5, ypt5p, has been identified recently (Armstrong et al., 1993). However, no experimental data are yet available that suggest any function for this protein in endocytosis in the fission yeast (Armstrong et al., 1993).

Here we report the isolation of three genes from the budding yeast *S. cerevisiae* that encode Ypt proteins with extensive homology to mammalian rab5 and the *S. pombe* ypt5p. The defects associated with single, double, and triple null mutants of *YPT51*, *YPT52*, and *YPT53* suggest an important function of the encoded proteins in the delivery to the vacuole of two endocytic markers, α-factor and LY. Furthermore, due to a number of vacuole-associated defects found for the here described *ypt* mutants, such as protein sorting, acidification and morphological changes, a requirement of these Ypt proteins for vacuole biogenesis can be envisaged.

Materials and Methods

Plasmids, Strains, and Growth Conditions

The yeast genomic library, kindly provided by M. Hall (Heitman et al., 1991), contains ~5–10 kb fragments resulting from partial digestion of *S. cerevisiae* genomic DNA with *Sau*3A (strain MH145-4B [Δ*{mat}130-141::CAN1-14, mfa2-lacZ, rme, ura3, leu2, his4, met, ade6, HMLa*]). The fragments were inserted into the BamHI site of the polylinker of plasmid pSEY8, a high-copy number 2 μm *URA3* vector (Emr et al., 1986).

pSEY8-BS6 and pSEY8-HSVI are isolated plasmids, originating from the genomic library described above, containing the *YPT51* and *YPT53* gene, respectively. Cosmid pUKG047 carrying the CEN11 region of *S. cerevisiae* was obtained from B. Dujon (Unité de Génétique Moléculaire des Levunes, Institut Pasteur, Paris) for systematic sequence analysis in the yeast genome sequence project of the European Community.

The *Escherichia coli* strains used in these experiments were MH1 (araD139, Δlac X74, galE, galK, hsr, rpsL) (provided by M. Hall, Biocenter, Basel, Switzerland), SE10 (Achstetter et al., 1988), and XL1-Blue (Stratagene, La Jolla, CA), which were grown in LB medium (1% NaCl, 1% peptone, 0.5% yeast extract). LB plates contained additionally 2% agar. Strains carrying plasmids were grown in the presence of 100 μg/ml ampicillin.

The strains of *S. cerevisiae* used in these experiments are listed in Table I. Unless otherwise indicated yeast strains were grown in complete medium (1% yeast extract, 2% peptone, and 2% glucose) (YPD) to early logarithmic phase (0.5–2 × 10^7 cells/ml) at 24°C on a rotary shaker. Synthetic growth medium (SD medium) has been described elsewhere (Dulic et al., 1991).

Reagents

^{35}S-labeled α-factor was prepared from biosynthetically labeled yeast cells overproducing the pheromone (Dulic et al., 1991). LY-CH was purchased from Fluka (Buchs, Switzerland), quinacrine was from Sigma Chemical Co. (St. Louis, MO), and carboxydichlorofluorescein diacetate (CDCFDA) was from Molecular Probes Inc. (Eugene, OR). Yeast tRNA, herring sperm DNA, dNTPs and ddNTPs were obtained from Boehringer Mannheim (Mannheim, Germany). Sequenase Version 2.0 was from United States Biochem. corp. (Cleveland, OH). ^{35}S-H_2SO_4 (carrier free), [^{35}S]methionine, α^{35}S-dATP, and α^{32}P-dCTP were purchased from Amersham Intl. (Buckinghamshire, England). Klenow-enzyme was from Boehringer Mannheim. Protein A-Sepharose CL-4B and Sepharose CL-4B were from Pharmacia (Uppsala, Sweden). Chemicals for gel electrophoresis were obtained from Bio Rad Laboratories (Richmond, CA) and National Diagnostics (Atlanta, GA). ENTENSIFY used for fluorography was from Dupont-NEN (Boston, MA).

Table I. Strains Used

Yeast strain	Genotype	Source
RH144-3D	*Mata his4 ura3 leu2 bar1-1*	H. Riezman
RH448	*Mata his4 ura3 leu2 lys2 bar1-1*	H. Riezman
RH1201	*Mata/α his4/his4 ura3/ura3 leu2/leu2 lys2/lys2 bar1-1/bar1-1*	H. Riezman
RH1606	*Mata his4 ura3 vat2::LEU2 ade6 bar1-1*	H. Riezman
BS2	*Mata his4 ura3 ypt53::LEU2 lys2 bar1-1*	this study
BS4	*Matα his4 ura3 ypt53::LEU2 lys2 bar1-1*	this study
BS13	*Mata his4 ypt52::URA3 leu2 lys2 bar1-1*	this study
BS14	*Matα his4 ypt52::URA3 leu2 lys2 bar1-1*	this study
BS17	*Mata his4 ypt52::URA3 ypt53::LEU2 lys2 bar1-1*	this study
BS25	*Mata his4 ura3 leu2 ypt51::LYS2 bar1-1*	this study
BS27	*Matα his4 ura3 leu2 ypt51::LYS2 bar1-1*	this study
BS40	*Mata his4 ura3 ypt53::LEU2 ypt51::LYS2 bar1-1*	this study
BS45	*Matα his4 ura3 ypt53::LEU2 ypt51::LYS2 bar1-1*	this study
BS48	*Matα his4 ypt52::URA3 leu2 ypt51::LYS2 bar1-1*	this study
BS57	*Mata his4 ypt52::URA3 leu2 ypt51::LYS2 bar1-1*	this study
BS62	*Mata his4 ypt52::URA3 ypt53::LEU2 lys2 bar1-1*	this study
BS63	*Matα his4 ypt52::URA3 ypt53::LEU2 ypt51::LYS2 bar1-1*	this study
BS64	*Mata his4 ura3 leu2 lys2 bar1-1*	this study
BS70	*Mata his4 ypt52::URA3 ypt53::LEU2 ypt51::LYS2 bar1-1*	this study

PCR Amplification of Ypt51 and Ypt53 Fragments and Isolation and Sequencing of Full Length Clones

Degenerate primers representing the protein sequence motif GXXXXGKS/T (Chavrier et al., 1992) and LAPMYYR [GT(G/T)GC(G/T)CC(G/T)AC-(G/T)AC(G/T)TAT(C/A)G(G/T)GAGAATGATAATAT] found in rab5A, rab5B, rab5C (Chavrier et al., 1992; Simons and Zerial, 1993) were used for amplification of yeast genomic DNA prepared from the strain RH144-3D. The initial PCR reaction was carried out in a volume of 20 μl and consisted of 30 cycles of 1 min each at 94°C, 2 min at 60°C, and 1 min at 72°C, with a final 5 min extention at 72°C. The reaction volume was increased to 100 μl and a second round of amplification was performed using the same conditions as described above. The reaction product of ~200 bp was gel purified and labeled with α^{32}P-dCTP (3,000 Ci/mmol) using the random primer labeling kit (Boehringer Mannheim). To isolate full length clones of the respective genes, ~40,000 *E. coli* colonies (transformed with the genomic library) were screened with the ^{32}P-labeled PCR reaction product. Plating of bacteria onto nitrocellulose filters on LB-Ampicillin plates and preparation of replica-filters were done by standard procedures (Sambrook et al., 1989). After lysing the cells with base and baking the filters for 2 h at 80°C, they were extensively washed with 3× SSC, 0.1% SDS at 68°C to remove bacterial debris. Prehybridization was performed for 2 h at 68°C in 6× SSC, 5× Denhard's solution, 100 μg/ml herring sperm DNA and 0.5% SDS. Hybridization was done for 12 h at 68°C in 6× SSC, 1× Denhard's solution, 100 μg/ml yeast tRNA and ^{32}P-labeled PCR reaction product at approximately 3 × 10^5 cpm/ml. Filters were washed with 2× SSC, 0.1% SDS at 68°C four times for 15 min and exposed wet against x-ray films (XAR5; Eastman Kodak Co., Rochester, NY). All positive clones identified in the initial screening were isolated and streaked out to obtain single colonies. 5–10 of these colonies were subjected to a second round of screening (as described above). Positive clones were restreaked and single colonies were subjected to a third round of rescreening as described above. Plasmids were isolated from the positive clones using Qiagen columns (Diagen, Düsseldorf, Germany) as described by the manufacturer.

To determine the nucleotide sequences of the respective clones, a degenerate oligonucleotide, representing a protein sequence motif that can be found in most Ypt/rab proteins, was used as a primer in dideoxy sequencing of double-stranded plasmid DNA. Sequencing was done according to the method of Winship (1989) using Sequenase Version2. This revealed that out of the 15 clones isolated, nine represented *YPT51* (four different subclones), three represented *YPT53* (one subclone), and three represented so far unidentified clones (different subclones). The coding sequence of *YPT51* and *YPT53* were determined from both strands by using nested primers.

Disruption of YPT51, YPT52, and YPT53

Large internal parts of the genes *YPT51*, *YPT52*, and *YPT53* were deleted from the genome and replaced with the *LYS2*, the *URA3*, and the *LEU2* gene, respectively. Using the polymerase chain reaction (PCR), the genomic flanking regions on either side of *YPT51* were amplified from pSEY8-BS6 to generate a 205-nucleotide fragment corresponding to the 5′ flanking region (5′FR) (nucleotides 385–589) and a 267-nucleotide fragment corresponding to the 3′ flanking region (3′FR) (nucleotides 1083 to 1349). The "inner" oligonucleotides, i.e., those immediately flanking the *YPT51* gene, were designed to create restriction sites for HindIII. The "outer" oligonucleotides contained restriction sites for ClaI (5′FR) and EcoRI (3′FR). The two PCR products were purified from an agarose gel and used as a template in a second round of PCR, which used as primers the two outer oligonucleotides used in the first PCR reactions. The major product of this reaction was digested with ClaI and EcoRI and subcloned into pBSK(−) (Stratagene). The resulting plasmid was opened with HindIII and a 4.7-kb *LYS2* fragment was ligated between the 5′FR and the 3′FR. Plasmid pBS-YPT51LYS2, containing the predicted insert, was linearized with ClaI and SmaI, the latter enzyme cutting ten nucleotides 3′ of the EcoRI site in the polylinker of pBSK(−), and used to transform the diploid strain RH1201 in a one step gene replacement (Orr-Weaver et al., 1981). After selecting for growth on plates in the absence of lysine, colonies were sporulated at 24°C. Tetrad dissection was then performed and the cells derived from different spores were grown up at 24°C and examined as described below.

The disruption of *YPT53* was performed by the same strategy as described for *YPT51*. The genomic flanking regions on either side of *YPT53* were amplified from pSEY8-HSVI to generate a 196 nucleotide 5′FR (nucleotide 418 to 613) and a 206 nucleotide spanning 3′FR (nucleotide 1150 to 1355). The inner oligonucleotides were designed to create restriction sites for XhoI, the outer oligonucleotides contained restriction sites for BamHI (5′FR) and PstI (3′FR). After two rounds of PCR (see above) the reaction product was subcloned into pGEM1 (Promega Corp., Madison, WI), opened with XhoI and a 2.2-kb XhoI/SalI fragment containing the *LEU2* marker was introduced. The resulting plasmid (pGEM-YPT53LEU2) was linearized with BamHI and PstI. Transformation and dissection of Leu$^+$ transformants was carried out as described above.

To create a loss-of-function allele of *YPT52*, a 2.4-kb *YPT52*-containing genomic fragment resulting from exonuclease/XbaI digest was subcloned into pBSK(−) to generate pBS-YPT52 and a 799-nucleotide EcoRV/EcoRV fragment containing the entire coding sequence of the gene was replaced by a 1.2-kb HindIII/HindIII fragment containing the *URA3* gene. The resulting plasmid (pBS-YPT52URA3) was linearized with KpnI (contained in pBSK) and XbaI and used for subsequent transformation of diploids.

The null alleles of *YPT51* and *YPT53* contained a deletion of codon 31 to 195 (inclusive) and codon 31 to 209 (inclusive), respectively. The null allele of *YPT52* did not contain any coding sequence information.

To determine integration of the respective constructs by site-specific recombination, DNA was prepared from cells derived from the four spores of complete tetrads was prepared (Philippsen et al., 1991). PCR was performed with a primer of the respective oligonucleotide that binds 5′ from the sequence that was used for homologous recombination of the three respective genes and a primer that binds to sequences within the 5′ region of the respective marker genes. With the mutants, amplification of a corresponding DNA fragment indicated that the marker gene integrated at its proper location, whereas with wild-type DNA no such amplification occurred. Additionally, Southern hybridization was performed with wild-type and mutant strains to confirm proper integration of the respective marker genes. For this, chromosomal DNA of the various strains was digested with EcoRI, separated on 0.8% (to analyze disruption of *YPT51* and *YPT53*) or 0.6% (to analyze disruption of *YPT52*) agarose gels and transferred to GeneScreen Plus membranes (Dupont-NEN) as suggested by the manufacturer. Probes for *YPT51* and *YPT53* were prepared by PCR, using the respective outer oligonucleotides described before, gel purified, and labeled with digoxigenin as suggested by the manufacturer (Boehringer Mannheim). To analyze disruption of *YPT52* two probes were prepared: a digoxigenin-labeled EcoRV/EcoRV fragment containing the coding region of *YPT52*, and a KpnI/BglII fragment containing the 5′ non-coding region of *YPT52*. Prehybridization and hybridization of probes with the filter and detection using anti-digoxigenin Fab fragment labeled with alkaline phosphatase was performed according to the protocol provided by Boehringer Mannheim. Correct integration and disruption of the respective *YPT* genes were indicated by the following results: replacement of a ~5-kb *YPT51* fragment in the wild type by a ~9-kb fragment in the *YPT51*-disrupted strain; appearance of a ~6.8- and 3.1-kb fragment in a *ypt53* mutant versus an ~8.6-kb fragment in the wild type strain; appearance of a ~8.2-kb fragment in a *ypt52* mutant versus a ~7.8-kb fragment in the wild-type strain using the KpnI/BglII probe, or disappearance of the 7.8-kb band in the *ypt52* mutant using the EcoRV/EcoRV *YPT52* probe.

α-Factor Internalization and Degradation Assays

Pheromone internalization and degradation assays were carried out as described by Dulic et al. (1991), using biosynthetically labeled ^{35}S-α-factor. Both assays were performed with the various strains grown overnight at 24°C. Binding of the pheromone was done for 1 h on ice, internalization at 30°C. The disappearance of intact, internalized α-factor (pH 1.2 sample) was quantified by densitometric scanning as described (Singer and Riezman, 1990).

LY-CH Accumulation

LY internalization experiments were essentially performed as described by Dulic et al. (1991). The various strains were grown to early logarithmic stage overnight at 24°C and LY accumulation (using 16 mg/ml final concentration) was analyzed after internalization at 30°C for 1 h. The cells were observed using a Zeiss Axiophot microscope equipped with fluorescence and Nomarski optics. Photographs were made using Kodak T-Max 400 films (Eastman Kodak Co.) exposed to ASA 1,600. Exposures for fluorescence were 30 s. To quantify the results obtained with *ypt52ypt53* mutants as compared with wild type, cells with a clear vacuolar staining positive for LY were counted as positive, cells without vacuolar staining, but with recognizable vacuole by Nomarski were counted as negative. 150 cells were counted.

Staining of Vacuoles with Quinacrine and CDCFDA

The different strains used for the analysis were grown overnight at 24°C to early logarithmic phase. For staining with quinacrine, 5×10^6 cells were collected and resuspended in 500 μl YPD, 50 mM Na_2HPO_4, pH 7.6. Quinacrine was added to 0.2 mM final concentration and staining was performed at RT for 5 min. The cells were washed once in 2% glucose, 50 mM Na_2HPO_4, pH 7.6, and immediately viewed on concanavalin A–coated coverslips as described by Roberts et al. (1991), using fluorescence and Nomarski optics. Photographs were made using Kodak T-Max P3200 films and exposures for fluorescence were done for 30 s.

For staining with carboxydichlorofluorescein diacetate (CDCFDA), 10^7 cells were resuspended in 100 μl SD medium, 50 mM citric acid, pH 5, 20 mM CDCFDA. After 20 min at 30°C the cells were immediately viewed using either the Axiophot microscope or, alternatively, the EMBL confocal microscope (excitation wavelength 476 nm). Photographs were made using Kodak T-Max 400 films exposed to ASA 1,600 (Axiophot) and Kodak T-Max 100 films (confocal microscpe). Exposures for fluorescence were 30 s except for analysis of *ypt51ypt52* and *ypt51ypt52ypt53* mutants for which the exposure was reduced to 5 s.

Thin Section Electron Microscopy

Electron microscopy of cells that had been grown at 30°C to early logarithmic phase was performed as described previously by Ossig et al. (1991).

Carboxypeptidase Y and Alkaline Phosphatase Biogenesis

Cells of the various strains used in the analysis were grown overnight at 24°C in YPD medium to ~1 × 10^7 cells/ml. Cells (5×10^7 per time point) were harvested, washed two times with H_2O and resuspended to 2.5×10^6 cells/ml in SD medium containing 2% glucose, 100 μM ammonium sulfate and nutrient supplements (SD low sulfate). After incubation at 24°C for 5 h the cells were collected, washed once with H_2O and resuspended to 2.5×10^7 cells/ml in minimal medium as described above, but without sulfate (SD no sulfate) and with 0.5 mg/ml bovine serum albumin.

To label whole cells, a pulse was initiated at 30°C by the addition of [^{35}S]methionine (40 μCi/time point, 1 mCi/66 μl) and metabolic labeling conducted for 5 min at 30°C. 1 ml of cells was removed (and processed as described below), ammonium sulfate was added to 2 mM, and methionine and cysteine to 30 μg/ml, each, to initiate the period of chase. 1-ml samples were taken after 2.5, 5, 10, 20, 40, and 60 min. To terminate the reaction, the 1-ml samples were added to NaN_3 and NaF (final concentration 5 mM each) and transferred to −20°C. Finally, the cells were thawed and TCA was added to 6% final concentration and protein was precipitated on ice for 30 min. The precipitates were collected by centrifugation, washed twice with −20°C acetone and dried. After addition of 100 μl of 50 mM Tris, pH 6.8, 1% SDS, 2.5 mM EDTA (lysis buffer) and acid-washed glass beads cell extracts were prepared at 4°C by vortexing for 1 min at top speed. The extracts were clarified by centrifugation and the supernatant was heated at 95°C for 5 min. After centrifugation for 5 min in a microcentrifuge, the supernatant was diluted with 1 ml TNET [1% (wt/vol) Triton X-100, 150 mM NaCl, 5 mM EDTA, 50 mM Tris/HCl, pH 8] and 1× CLAP (5 μg of each chymostatin, leupeptin, antipain and pepstatin, prepared from a 1,000X stock in DMSO). To remove material that binds nonspecifically to protein A–Sepharose beads, 100 μl of a 1:2 slurry of Sepharose CL-4B in TNET was added and incubated for 1 to 2 h on a rocker at 4°C. The unbound material was transferred to a fresh tube. For immunoprecipitation, 3 μl of anti–carboxypeptidase Y (CPY) antiserum and 50 μl of a 1:2 slurry of protein A–Sepharose CL-4B in TNET was added and incubated with the labeled extracts overnight at 4°C. After collecting the beads by centrifugation, the supernatant of each reaction was subjected to immunoprecipitation with anti–alkaline phosphatase (ALP) antibodies for 5 h at 4°C. The beads containing the anti-CPY immunocomplexes were washed five times with 1 ml TNET and resuspended in 60 μl Laemmli sample buffer. The beads containing the anti-ALP immuncomplexes were washed once with TNET, once with 2 M urea, 2 M NaCl, 1% TX100, 100 mM Tris/HCl, pH 6.8, once with TNET, and twice with 10 mM Tris/HCl, pH 6.8, 10 mM NaCl. The immunoprecipitates were released from the beads at 95°C for 5 min and separated by SDS-PAGE under reducing conditions using 8% gels. After electrophoresis the gels were fixed, treated with ENTENSIFY according to the manufacturer's instructions, dried and exposed to films at −70°C for 5 (CPY immunoprecipitation) or 14 (ALP immunoprecipitation) days.

To determine extracellular secretion of vacuolar enzymes, cells (2×10^8 cells/ml) were treated in 0.1 M Tris/HCl, pH 6.8, 0.14 M cysteamine, 1.2 M sorbitol, 5 mM EDTA for 15 min at 30°C after incubation in SD low sulfate for 5 h as described above. 10^8 cells were collected and converted into spheroplasts in a volume of 90 μl of SD no sulfate, 0.1 M Tris, pH 6.8, 1.2 M sorbitol, 1 mg/ml each of BSA and ovalbumin and 10 μl lyticase. After incubation at 30°C for 45 min, the spheroplasts were collected by centrifugation for 5 min at 1,500 rpm, resuspended in the same medium except for lyticase, and pulse labeling was initiated by the addition of 6 μl [^{35}S]methionine (1 mCi/66 μl). After 15 min at 30°C, a chase period of 30 min followed as described above. The reaction was stopped by the addition of NaN_3 and NaF to 5 mM final concentration, each, and by chilling the spheroplasts to 4°C. The spheroplasts were collected by centrifugation for 10 min at 1,500 rpm and the supernatant was withdrawn. Both, medium and spheroplasts, that were resuspended in the medium used for labeling, were frozen and processed for successive immunoprecipitation with anti-CPY and anti-ALP antibodies as described above. Quantitation was performed on short exposures of fluorograms by densitometric scanning. The values for p2CPY and mCPY in the intracellular and extracellular fraction were added and considered as 100% total.

Cell extracts from overnight cultures grown at 24°C were prepared by collecting cells (50 OD units), washing them once with water and resuspending them to 1-2 OD/ml in 0.2N NaOH, 0.5% β-mercaptoethanol. After a 10-min incubation on ice, TCA was added to 10% final concentration and proteins were precipitated on ice for 30 min. The precipitates were collected by centrifugation, washed once with cold acetone and resuspended in Laemmli sample buffer (10 OD/ml). After SDS-PAGE on 8% gels the proteins were transferred to nitrocellulose membranes (Towbin et al., 1979). Western blot analysis was performed according to Singer and Riezman (1990). The antiserum against CPY was used 1:1,000 diluted. Secondary goat anti-rabbit IgG conjugated to horseraddish peroxidase was used 1:3,000 diluted and detected with the ECL system (Amersham).

Results

Identification of Three S. cerevisiae Genes, YPT51, YPT52, and YPT53, That Encode Proteins with Extensive Homology to rab5 and S. pombe ypt5p

Mammalian cells express rab5A (to which we refer as rab5) and two isoforms, rab5B and rab5C (Chavrier et al., 1992; Bucci, C., A. Lütcke, V. Olkkonen, P. Dupree, K. Simons, and M. Zerial, manuscript in preparation) which share sequence identity in the range of 85%. Recent data indicate that, similar to rab5, rab5B and rab5C regulate trafficking in the early endocytic pathway. To identify putative homolog(s) of rab5 in *S. cerevisiae* we first searched for an amino acid sequence motif specific for the rab5 subgroup. Comparative analysis of all the available protein sequences revealed that the LAPMYYR motif is shared by all three mammalian rab5 proteins whereas it is absent from all other rab/Ypt proteins. This sequence is located within the helix α2 of small GTPases (nomenclature according to Pai et al., 1989), which is highly conserved between mammalian rab proteins and their yeast counterparts, such as rab1A, rab1B and Yptlp, and which contributes to the functional specificity of rab5 (Stenmark et al., 1994). Two degenerate oligonucleotides corresponding to the LAPMYYR sequence and to the GXXXXGKS/T motif found in the phosphate-binding loop of all rab/Ypt proteins (Chavrier et al., 1992) were used in the polymerase chain reaction (PCR) to amplify a putative *YPT5* gene(s) from *S. cerevisiae* genomic DNA. As determined by Southern blot analysis, upon labeling with ^{32}P, the PCR reaction products hybridized to two distinct genomic DNA fragments (not shown). The respective full-length clones were isolated from a genomic library and shown to represent two novel sequences. Analysis of the two identified clones revealed two intronless genes encoding small GTPases of the

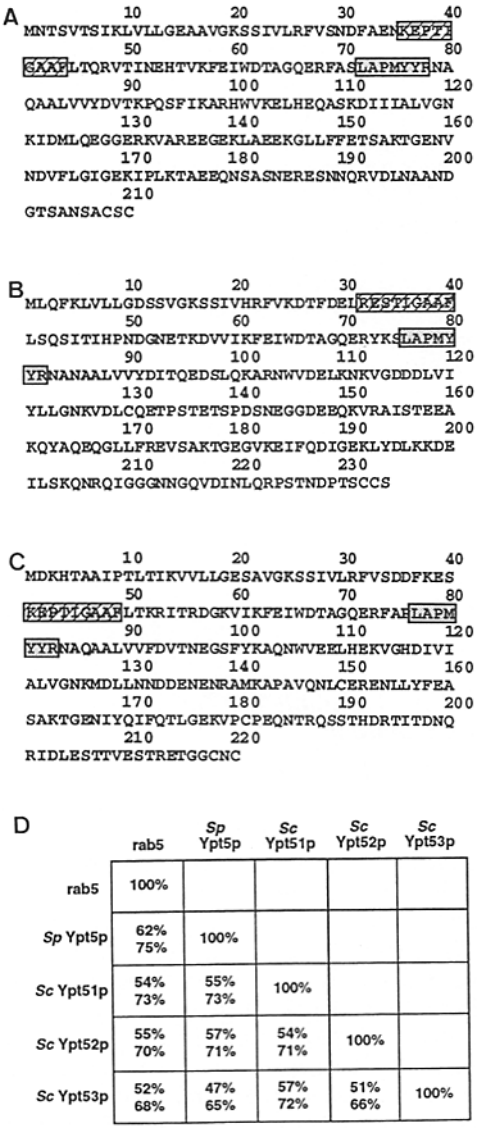

Figure 1. Amino acid sequence of Ypt51p (*A*), Ypt52p (*B*) and Ypt53p (*C*) and numbers of identity/homology shared between rab5 and Ypt proteins (*D*). The boxed clear regions in *A*, *B*, and *C* represent the α2 domain, the hatched segments correspond to the effector domain (see Results). The nucleotide sequence data are available from EMBL/GenBank/DDBJ under the accession numbers X76173 SCYPT51, X76174 SCYPT52, and X76175 SCYPT53, respectively. In *D*, the values of identity (*upper figure*)/homology (*lower figure*) for the different protein pairs were determined by the gap program of the GCG package.

rab/Ypt protein family (Fig. 1) with the closest identity and phylogenetic relationship to rab5 and *S. pombe* ypt5p (data not shown). Based on these features, but in keeping with the conventional nomenclature used for *S.cerevisiae* genes, the two genes were named *YPT51* and *YPT53* (see below). Independently, sequencing of the *S. cerevisiae* chromosome XI revealed an open reading frame, that codes for another protein with a high sequence homology to rab5, but which was distinct from *YPT51* and *YPT53*. This gene was subsequently named *YPT52* (Fig. 1). Although *YPT52* contains the nucleotide sequence encoding the LAPMYYR motif, it was not identified by the PCR approach. This can probably be explained by three mismatches at the 3′ end of the degenerate oligonucleotide representing the GXXXXGKS/T motif. Because all gene products were equally similar to rab5, the gene with the major importance in respect to phenotypic alterations (see below) was called *YPT51*, followed by *YPT52* and *YPT53*.

The overall sequence identity/homology between all possible pairs of rab5/Ypt proteins was very similar and in the range of 54% identity and 70% homology, respectively. Computer analysis of all available rab/Ypt protein sequences to calculate their phylogenetic relationship revealed that mammalian rab5A, B, and C, *S. pombe* ypt5p and *S. cerevisiae* Ypt51p, Ypt52p and Ypt53p constitute a group among the members of this family (data not shown). Further support for their close relationship is provided by the striking similarity in the effector domain, which in the case of $p21^{ras}$ is known to mediate interactions with the GTPase-activating protein (Adari et al., 1988; Cales et al., 1988). Ypt52p and *S. pombe* ypt5p contain identical effector domains (RESTIGAAF) (Fig. 1), which differ from rab5 in only one amino acid. Ypt51p and Ypt53p, which contain identical effector domains, have two amino acid differences when compared with Ypt52p and rab5, respectively (Fig. 1).

Analysis of the codon usage, which is a reliable indicator of protein abundance in yeast (Bennetzen and Hall, 1982), revealed that on a scale in which 1 represents exclusive use of preferred codons, *YPT51* scored 0.18, *YPT52B* scored 0.23, and *YPT53* scored 0.07. This suggests that *YPT53*, most likely, encodes an extremely rare protein, whose putative low abundance is slightly above that of transcription factors (0–0.05), whereas *YPT51* and *YPT52* encode proteins which lie in the typical range of other Ypt proteins, like Ypt7p (0.14) and Sec4p (0.21).

These data indicate that *S. cerevisiae YPT51*, *YPT52*, and *YPT53* are novel sequences which code for small GTPases sharing structural features with mammalian rab5A, B, and C proteins.

Disruption Of YPT51 And YPT52 Has a Synergistic Inhibitory Effect on Cell Growth

To determine the function of Ypt51p, Ypt52p, and Ypt53p, we first constructed mutants with null alleles of *YPT51*, *YPT52*, and *YPT53* alone, all possible pairs of double mutants and the triple *ypt51ypt52ypt53* null mutant. To generate single null mutants the disrupted genes and a selectable marker on a linear fragment were used to replace the respective wild-type genes in diploid strains, that were auxotrophic for the different markers. After sporulation and tetrad dissection it was observed that haploid progeny carrying either wild-type or the disrupted gene for *YPT51*, *YPT52*, or *YPT53* formed colonies of similar size after growth at 24°C, suggesting that all three *YPT* genes are non-essential. All possible combinations of double mutants and the triple mutant were obtained by crossing haploid null mutants, followed by tetrad dissection of the respective diploids. The haploid double and triple mutants also did not show any growth defect upon incubation at 24°C. However, when precultures of wild-type and mutant cells grown at 24°C were diluted into YPD medium at 37°C, *Δypt51* mutants were delayed in growth, whereas *Δypt52* and

Δypt53 mutants propagated like wild-type cells (Fig. 2 *A*). Disruption of *YPT53* in combination with *YPT51* or *YPT52* did not change the growth properties of the latter two single mutants (Fig. 2 *B*). In contrast, in the double *ypt51ypt52* mutant growth was further inhibited at 37°C (Fig. 2 *B*) as compared with the single *ypt51* null mutant, and a mild delay of growth could already be observed at 30°C (not shown). The triple *ypt51ypt52ypt53* mutant was viable and had similar growth properties to the double *ypt51ypt52* mutant (compare Fig. 2 *B* with *A*).

ypt51, ypt52, and ypt53 Mutants Internalize α-Factor Normally, but Are Defective in Pheromone Degradation

To investigate a possible role of the three Ypt proteins in endocytosis, the internalization of the mating pheromone α-factor was analyzed. ^{35}S-α-factor internalization assays were performed at 30°C with cells that had been grown at 24°C. At those temperatures no major growth defects could be observed, which might negatively influence the assay. The results showed that none of the mutants were defective for α-factor binding and internalization (data not shown). Both the rate of internalization and the total amount of endocytosed pheromone in all three single and the triple null mutants were indistinguishable from wild-type cells.

The degradation of internalized α-factor was then analyzed by separating the intact and degraded forms of ^{35}S-labeled pheromone by thin layer chromatography. Similar to wild-type cells, that had completely degraded the pheromone after 30 min of internalization (Fig. 3 *A*), single null mutants of *YPT52* and *YPT53* degraded the pheromone with normal kinetics (data not shown). *ypt52ypt53* mutants revealed a minor delay in pheromone degradation, since small amounts of intact α-factor were still present after 30 min of incubation at 30°C (Fig. 3 *B*). In contrast, pheromone degradation was strongly inhibited in *ypt51* mutants (Fig. 3 *C*). The $t_{1/2}$ for α-factor degradation was prolonged to about 50 min as compared with 10 min in wild-type cells. *ypt51ypt52* (Fig. 3 *E*) and *ypt51ypt53* (Fig. 3 *D*) mutants displayed a further delay in α-factor degradation as compared to single *ypt51* mutants, with a $t_{1/2}$ of pheromone degradation of about 60 and 75 min, respectively. Triple *ypt51ypt52ypt53* mutants (Fig. 3 *F*) seemed to be almost blocked in pheromone degradation, since the $t_{1/2}$ was more than 120 min.

These results indicate that disruption of the *YPT51* gene does not affect α-factor internalization but causes a severe inhibition of pheromone degradation. Furthermore, this effect is aggravated by the additional disruption of *YPT52* and *YPT53*.

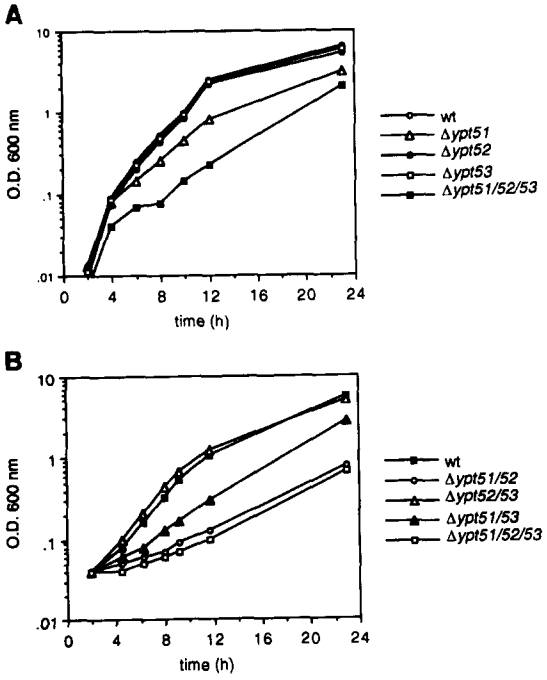

Figure 2. Growth curves of *Δypt51*, *Δypt52*, and *Δypt53* (*A*) and *ypt51ypt52*, *ypt51ypt53*, *ypt52ypt53*, and *ypt51ypt52ypt53* strains (*B*) as compared with wild-type cells. Precultures of the corresponding strains were grown to stationary phase at 24°C. To initiate growth the cells were diluted into YPD medium and incubated at 37°C. Aliquots were taken at the times indicated to measure the optical density at 600 nm.

ypt51, ypt52, and ypt53 Mutants Are Defective in Vacuolar LY Accumulation

The observed lack of pheromone degradation in the here described *ypt* mutants could be explained by an inhibition of transport from an endocytic compartment to the site of degradation, the vacuole. To test this hypothesis, we investigated the ability of the various mutants to deliver LY to the vacuole. As compared with wild-type cells (Fig. 4 *A*), single mutants for *YPT52* (Fig. 4 *B*) and *YPT53* (not shown) revealed no defect in the accumulation of the fluorescent dye in the vacuole. In contrast, *Δypt51* mutants were characterized by a strong reduction in the amount of LY accumulation in the vacuole (Fig. 4 *C*). The majority of cells showed a very weak or no detectable fluorescence in the region of the vacuole, which was generally recognizable by Nomarski optics. Only in rare cases did LY accumulate in the vacuole in similar amounts as observed for wild-type cells (Fig. 4 *C*). Interestingly, disruption of both *YPT51* and *YPT52* further decreased LY transport to the vacuole (Fig. 4, *E* and *F*), since even the occasionally observed weak fluorescence of vacuoles could not be detected. This phenotype was especially noteworthy in light of the fact that the majority of mutant cells contained the typically large vacuole, as seen in wild-type cells. Occasionally, cells of double as well as triple mutants revealed a remarkably bright intracellular fluorescence. This bright staining could sometimes be resolved into tiny spots (Fig. 4, *D*, *E*, and *F*, *arrowheads*). As detected by Nomarski optics, these particular cells did not contain a large vacuole like wild-type cells, but rather exhibited a granular surface similar to class C *vps* mutants lacking vacuoles (Banta et al., 1988). *ypt51ypt53* mutants appeared very similar to *ypt51* mutants, in that occasionally a weak vacuolar staining by LY could be observed (Fig. 4 *D*). However, in difference to the latter mutant a few cells showed the spotty fluorescence as described for the *ypt51ypt52* mutant (Fig. 4, *E* and *F*, *arrowheads*). Therefore, additional disruption of *YPT53* in *Δypt51* mutants resulted in a phenotype which was stronger than observed for *ypt51* and weaker than

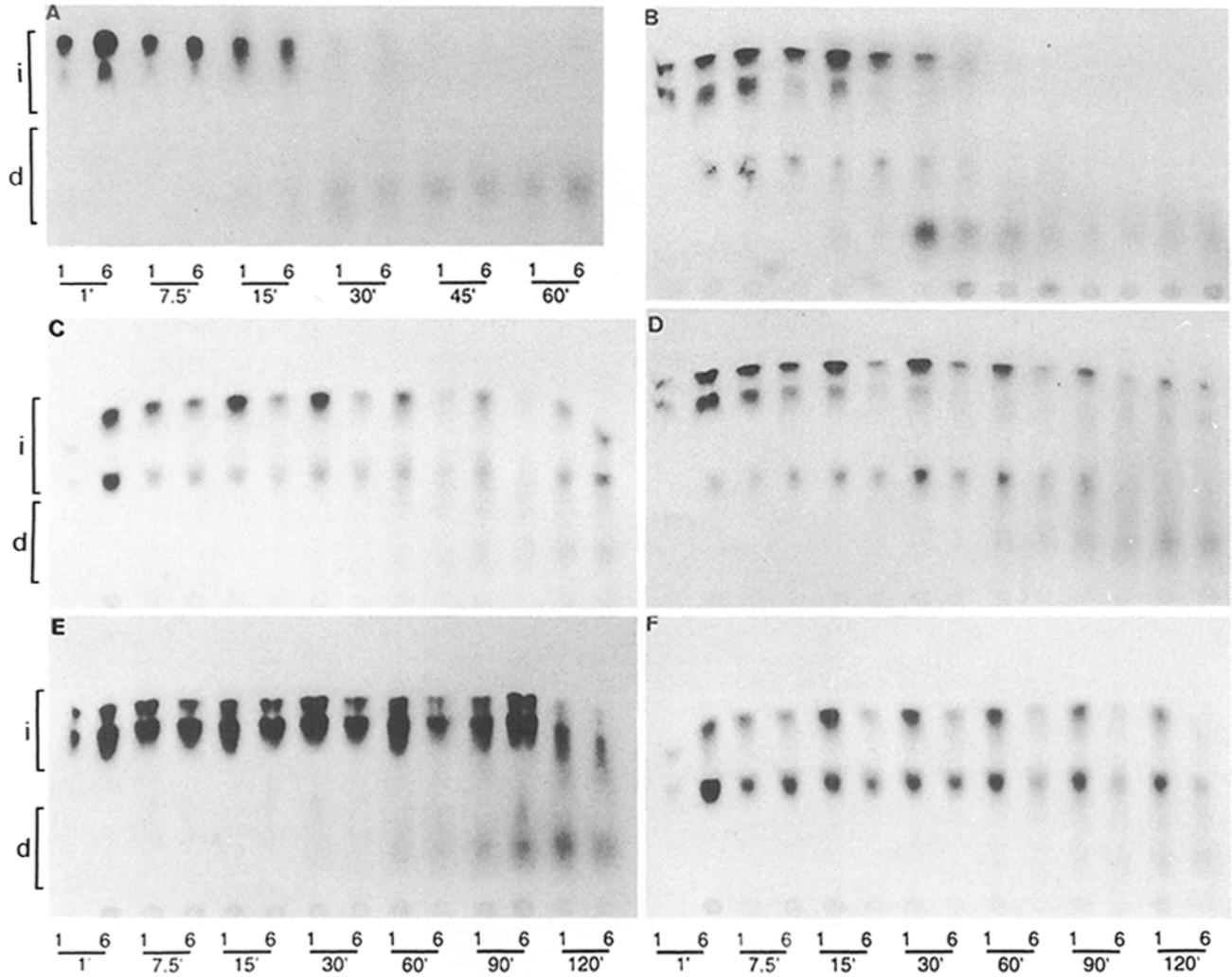

Figure 3. α-factor degradation by *ypt* mutants as compared to wild-type cells. α-cells of the respective strains were grown overnight at 24°C to early logarithmic stage. After incubation with ^{35}S-α-factor for 1 h at 0°C the cells were collected and resuspended in YPD medium and transferred to a 30°C waterbath to start internalization of the pheromone. Total cell-associated (pH 1.2 washed cells) (*1*) and internalized α-factor (pH 6 washed cells) (*6*) was extracted at the times indicated and resolved by thin layer chromatography. The positions of the intact (*i*) and degraded (*d*) pheromone are indicated. The fluorograms were exposed for 20 d at −70°C. *A*, wild type; *B*, *ypt52ypt53*; *C*, *ypt51*; *D*, *ypt51ypt53*; *E*, *ypt51ypt52*; *F*, *ypt51ypt52ypt53*.

observed for *ypt51ypt52* mutants. Although the majority of cells with a disrupted copy of both *YPT52* and *YPT53* showed no defect in LY accumulation (data not shown), it appeared that the number of cells without dye accumulation was increased as compared to wild-type cells. Whereas typically ~95% of wild-type, *ypt52* and *ypt53* cells revealed staining of the vacuole with LY, this number was reduced to about 50% in double *ypt52ypt53* mutants.

ypt51, ypt52, and ypt53 Mutants Display a Delay in the Maturation of a Soluble and a Membrane-bound Vacuolar Enzyme and also Partially Missort a Soluble Vacuolar Marker Protein

As in mammalian cells, the endocytic and the vacuolar sorting pathways in *S. cerevisiae* have been proposed to intersect in a prevacuolar, endosomal compartment (Vida et al., 1993; Schimmöller and Riezman, 1993; Davis et al., 1993). The finding that the here described Ypt proteins are required for transport of LY and possibly of α-factor to the vacuole suggests that delivery of enzymes to the vacuole via the secretory pathway could also be affected in the *ypt51*, *ypt52*, and *ypt53* mutants. To test this, transport of the vacuolar hydrolases carboxypeptidase Y (CPY) and alkaline phosphatase (ALP) to the vacuole was analyzed. The transit of soluble CPY through the secretory pathway can be monitored by the appearance of its different intermediate forms. Cleavage of the signal peptide and core glycosylation in the ER generate a 67-kD form, p1CPY, which is transported to the Golgi complex, where the core oligosaccharides are extended, yielding p2CPY (69 kD). Finally, just before or upon arrival of p2CPY in the vacuole the NH_2-terminal prosequence is removed to yield mature (m) CPY (61 kD) (Stevens et al., 1982) (Fig. 5). During biosynthesis of membrane-bound ALP, conversion of the 76-kD Golgi precursor (pALP) into

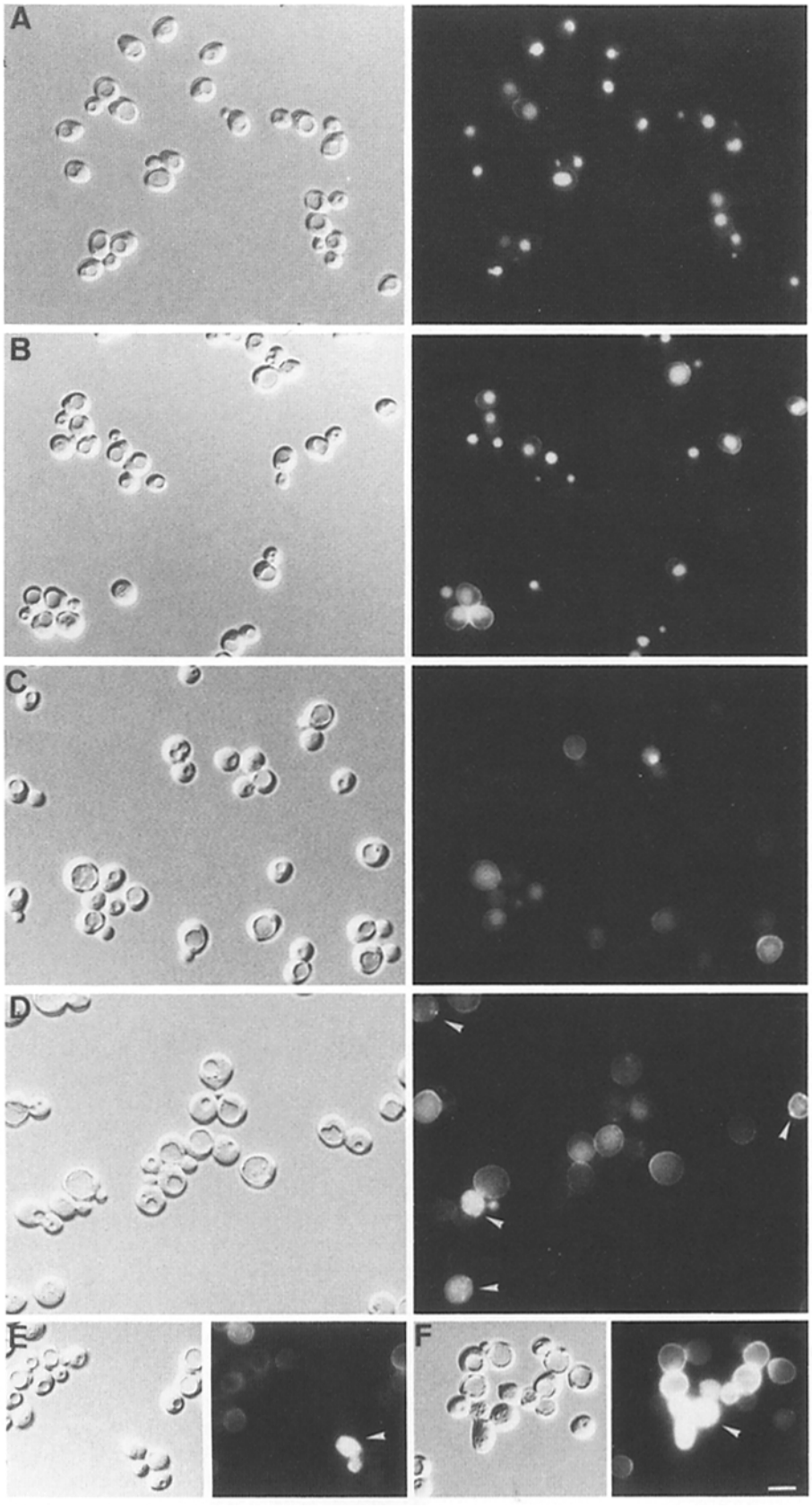

Figure 4. Accumulation of LY-CH by wild-type (*A*), *Δypt52* (*B*), *Δypt51* (*C*), *ypt51ypt53* (*D*), and *ypt51ypt52* (*E* and *F*) cells. After growth of cells overnight at 24°C to early logarithmic stage LY-CH internalization was performed at 30°C for 1 h. The cells were subsequently washed, mounted in low melting agarose, and visualized using Nomarski and fluorescence optics. Bar, 5 μm.

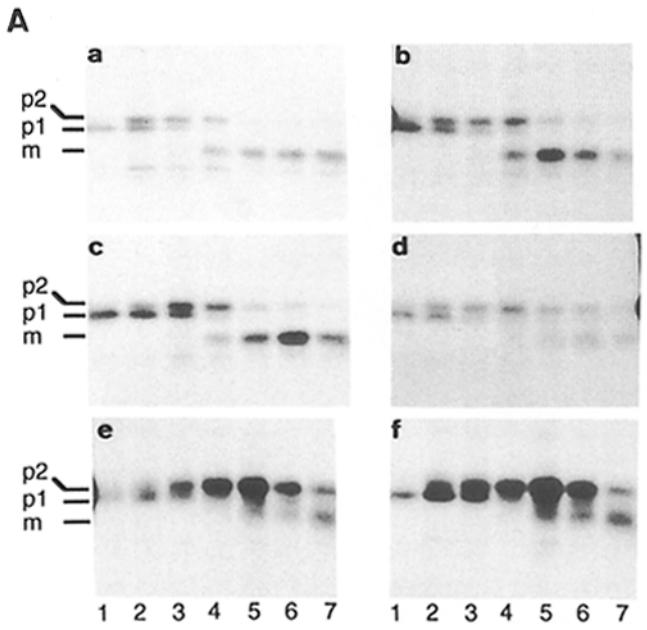

Figure 5. Carboxypeptidase Y biogenesis in *ypt* mutants and wild-type cells. Cells were labeled for 5 min at 30°C using [^{35}S]methionine and the chase was subsequently initiated by the addition of ammonium sulfate, unlabeled methionine and cysteine. At 0 (lane *1*), 2.5 (lane *2*), 5 (lane *3*), 10 (lane *4*), 20 (lane *5*), 30 (lane *6*), and 60 (lane *7*) min of chase aliquots of cells were removed and processed for immunoprecipitation with anti-CPY antibodies. Immunoprecipitates were analyzed on 8% gels by SDS-PAGE and fluorography. The fluorograms were exposed for 5 d at −70°C. *p*, precursor; *m*, mature form. Other background bands are nonspecific. *a*, wild type; *b*, *ypt52*; *c*, *ypt52ypt53*; *d*, *ypt51*; *e*, *ypt51ypt52*; and *f*, *ypt51ypt52ypt53*.

the 71-kD mature form (mALP) occurs in the vacuole by *PEP4*-dependent processing (Klionsky and Emr, 1989).

Pulse-chase labeling with [^{35}S]methionine was performed with cells that had been grown at 24°C. After a pulse of 5 min at 30°C, the cells were chased for various periods of time at 30°C, and the radioactive CPY and ALP were successively immunoprecipitated from total cellular protein and subsequently analyzed by SDS-PAGE. Conversion of pl to p2CPY and maturation to mCPY took place with normal kinetics in *Δypt52* (Fig. 5) and *Δypt53* (not shown) mutants as compared with wild-type cells. In *ypt52ypt53* double mutants, despite of a 5-min delay in the conversion from pl to p2 CPY, processing to the mature form occurred normally. Interestingly, *Δypt51* mutants exhibited a clear delay in the processing of p2 to mCPY. While in wild-type cells ~50% of p2CPY was processed to mCPY by 10 min of chase, in mutant cells a similar degree of processing was only observed after 20–30 min of chase. *ypt51ypt52* and *ypt51ypt52-ypt53* mutants were characterized by a further delay in this maturation step, since a chase of approximately 60 min was required to yield 50% of both p2 and mCPY (Fig. 5).

Maturation of membrane-bound ALP was also perturbed in mutant cells lacking Ypt proteins. However, while in *ypt51ypt52* and *ypt51ypt52ypt53* mutants 50% of mALP was formed only after 20 min, as compared with 5–10 min in wild-type cells, in all other mutants the processing of this protein took place with wild-type kinetics (data not shown). Thus, maturation of ALP appeared to be less severely perturbed in the here described *ypt* mutants than maturation of CPY.

In view of the observed delay in the maturation of vacuolar enzymes, the possibility had to be considered that a fraction of vacuolar enzymes is not properly sorted to the vacuole, but instead missorted to the extracellular space, a phenotype associated with a number of vacuolar protein sorting (*vps*) mutants (Robinson et al., 1988; Rothman et al., 1989*a*). To examine this, spheroplasts of the various mutants and of wild-type cells were pulse labeled for 15 min and chased for 30 min. After termination of the chase period by addition of NaN_3 and NaF, the intracellular and extracellular fractions were separated and two successive immunoprecipitations were performed with CPY and ALP antisera. As shown in Fig. 6 *A*, wild-type, *ypt52*, *ypt53* and *ypt52ypt53* cells contained mainly mCPY which was present in the intracellular fraction, suggesting proper targeting to the vacuole. In contrast, substantial amounts of Golgi-modified p2CPY (~40% of total) was found in the extracellular fraction of *Δypt51* mutants, providing evidence for missorting of this soluble enzyme. In fact, *vps21* (Robinson et al., 1988) is a mutant allele of *YPT51* (Emr, S., personal communication). Addi-

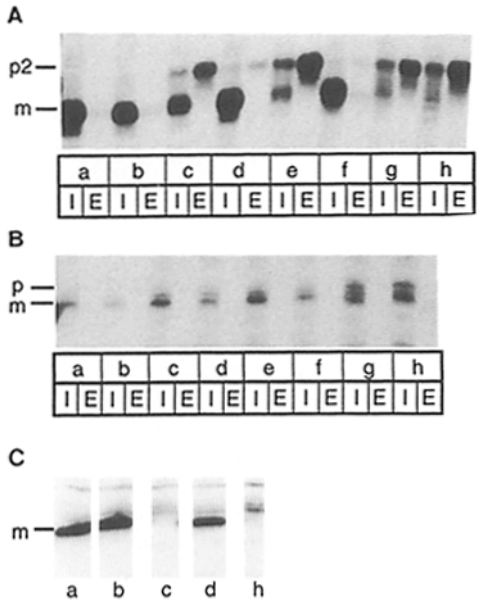

Figure 6. Sorting of the vacuolar enzymes CPY (*A*) and ALP (*B*) and steady state levels of mCPY (*C*). (*A* and *B*) Cells of the respective strains were converted into spheroplasts, labeled for 15 min with [^{35}S]methionine and chased for 30 min using conditions described in Fig. 8. To analyze secreted proteins the spheroplasts were separated from the medium by centrifugation at 1,500 rpm for 5 min. The cell and the medium factions were processed for successive immunoprecipitation using antibodies against CPY (*A*) and ALP (*B*). *I*, intracellular; *E*, extracellular; *p*, precursor; *m*, mature form. Other background bands are nonspecific. (*C*) Protein extracts of the various strains were prepared from overnight cultures grown at 24°C and separated by SDS-PAGE. Western analysis was performed with antibodies against CPY and the ECL detection system. *m*, mature CPY. *a*, wild type; *b*, *ypt53*; *c*, *ypt51*; *d*, *ypt52*; *e*, *ypt51ypt53*; *f*, *ypt52ypt53*; *g*, *ypt51ypt52*; *h*, *ypt51ypt52ypt53*.

tional disruption of either *YPT52* or *YPT53* increased the ratio of external to internal CPY suggesting enhanced missorting. Approximately 55 and 50% of total CPY was present extracellularly in *ypt51ypt52* and *ypt51ypt53* mutants, respectively. Furthermore, increasing amounts of intracellular p2CPY versus mCPY accumulated in *ypt51ypt53* and even more in *ypt51ypt52* mutants. The triple *ypt51ypt52ypt53* mutants displayed the highest degree of CPY missorting (~60% of total) and the strongest defect in precursor accumulation.

Although upon pulse-chase labeling of *ypt51ypt52* and *ypt51ypt52ypt53* mutants small but clearly detectable quantities of mCPY could be detected, as shown in Fig. 5, in the experiment of Fig. 6 *A* the amounts of mCPY seemed to be reduced in favor of increased quantities of p2CPY. This apparant discrepancy in the results most likely can be ascribed to the fact that spheroplasts on the one hand (more precursor accumulation) and intact cells on the other hand (less precursor accumulation) were used. A similar result was obtained in studies of vacuolar protein maturation with vacuolar acidification (*vat*) mutants (Klionsky et al., 1992).

As expected for a membrane protein, missorting of ALP to the extracellular medium could not be detected in any of the different *ypt* mutants (Fig. 6 *B*). As seen in pulse-chase labeling experiments (data not shown), precursor accumulation could be detected only in *ypt51ypt52* and *ypt51ypt52-ypt53* mutants.

We also determined the steady state levels of mCPY and mALP in the various mutants as compared with wild-type cells. This was done by Western analysis of protein extracts prepared from cultures grown overnight at 24°C. Surprisingly, *ypt51* mutants revealed no detectable amounts of mCPY as compared with wild-type cells and the other single *ypt* mutants (Fig. 6 *C*). This is in apparent contrast to the results obtained by pulse-chase labeling experiments, in which the generation of mCPY could clearly be observed in the *YPT51*-disrupted cells, and suggests a reduced stability of mCPY over longer periods of time. The steady-state levels of mALP were reduced to ~50% of wild-type levels in *ypt51* and *ypt51ypt52ypt53* mutants (data not shown).

To exclude the possibility that in the absence of Ypt51p, Ypt52p, and Ypt53p the secretory transport pathway was affected in a more general way, we also investigated the secretion efficiency of invertase and the mating pheromone α-factor. A comparison of wild-type cells with the different *ypt* null mutants revealed that both marker proteins were secreted with normal kinetics (data not shown).

In conclusion, while these results reveal no secretion defects and only slight perturbations of ALP maturation in *ypt51ypt52* and *ypt51ypt52ypt53* mutants, the kinetics of CPY maturation were increasingly impaired by the successive disruption of *YPT51*, *YPT52*, and *YPT53*, and missorting of CPY was simultanously increased. Furthermore, it appeared that the steady state level of mCPY was strongly reduced in *Δypt51* mutants.

Acidification Properties Are Disturbed in the Here Described ypt Mutants

In view of the missorting defect associated with some of the *ypt* mutants the possibility existed that this phenotype could be related to improper vacuole acidification. Precedents for this are a number of *vps* mutants (Banta et al., 1988; Preston et al., 1989; Rothman et al., 1989*b*) and specific mutants lacking subunits of the vacuolar ATPase (Nelson and Nelson, 1990; Preston et al., 1989; Yamashiro et al., 1990). Missorting of vacuolar enzymes can also be caused by raising the pH specifically of the vacuolar system by treatment with the drug bafilomycin A_1 (Banta et al., 1988; Klionsky and Emr, 1989). Vacuole acidification can be microscopically detected by staining living yeast cells with the lysosomotrophic agent quinacrine, a fluorescent dye that accumulates in acidified organelles (Weisman et al., 1987).

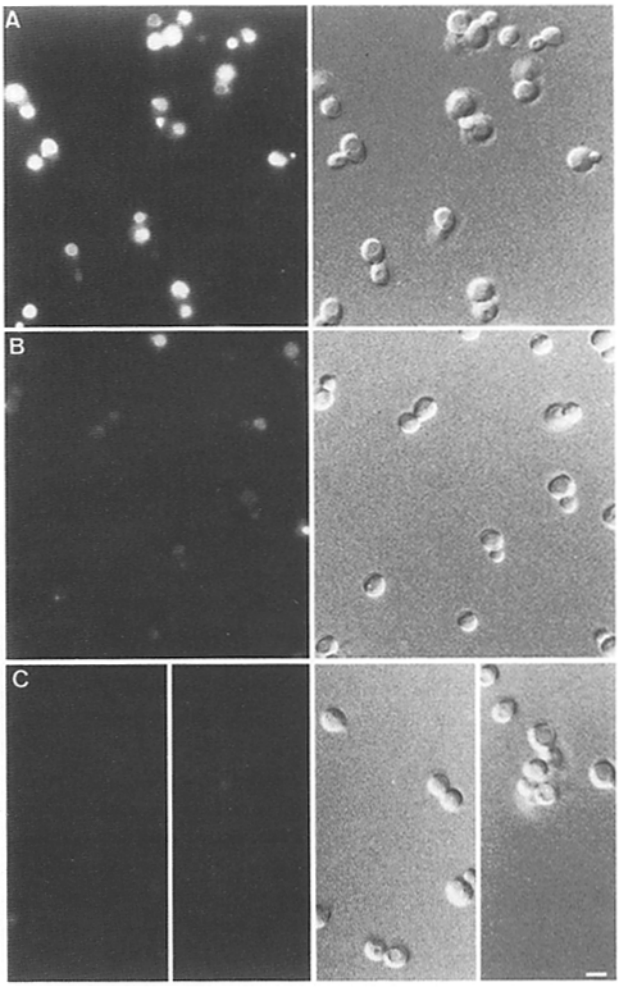

Figure 7. Vacuole acidification as determined by Quinacrine staining is defective in *ypt51* and *ypt51ypt52ypt53* mutants. Wild-type (*A*), *ypt51* (*B*) and *ypt51ypt52ypt53* (*C*) cells were grown at 24°C to early logarithmic phase and collected into YPD medium, 50 mM Na_2HPO_4, pH 7.6. Quinacrine was added and staining was performed for 5 min at room temperature. The cells were washed once in 2% glucose, 50 mM Na_2HPO_4, pH 7.6, and immediately viewed on concanavalin A-coated coverslips using Nomarski and fluorescence optics. Bar, 5 μm.

As shown in Fig. 7 *A*, wild-type cells revealed a bright vacuolar fluorescence, as did *ypt52*, *ypt53*, and *ypt52ypt53* null mutants (not shown). In contrast, this staining was strongly reduced in cells with a disrupted copy of *YPT51* (Fig. 7 *B*), and was virtually absent in *ypt51ypt52* (not shown) and *ypt51ypt52ypt53* mutants (Fig. 7 *C*). This clearly

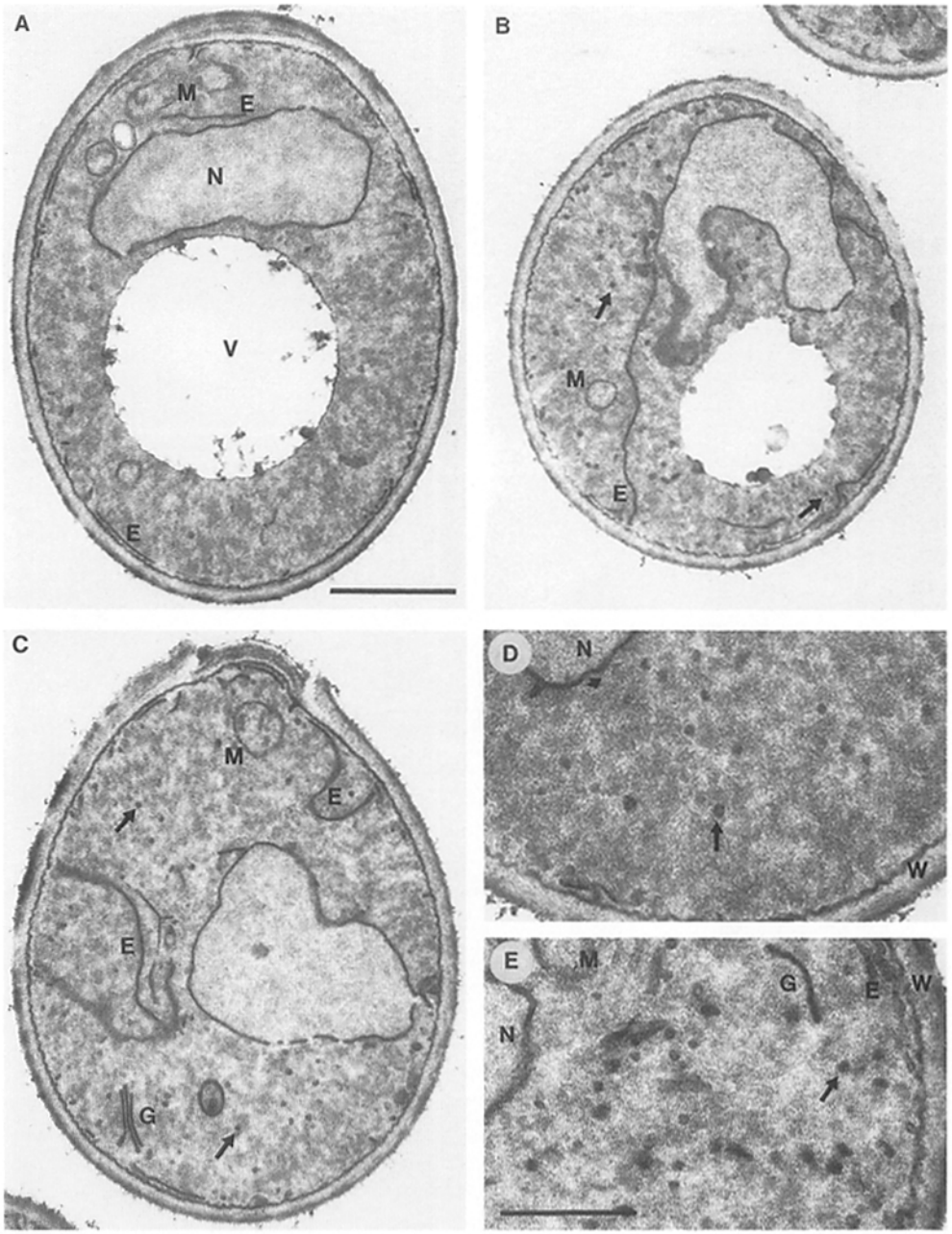

Figure 8. Accumulation of vesicular structures in Ypt51p-depleted cells. Wild type cells (*A*), *ypt51* (*B* and *D*), and *ypt51ypt52ypt53* (*C* and *E*) null mutants were fixed with potassium permanganate and viewed by thin section electron microscopy. Arrows point to 40–60-nm vesicles. *E*, endoplasmic reticulum; *G*, Golgi; *M*, mitochondria; *N*, nucleus; *V*, Vacuole; *W*, cell wall. Bars: (*A–C*) 1 μm; (*D* and *E*) 0.5 μm.

demonstrated that the absence of Ypt51p and Ypt52p results in a severe acidification defect of the vacuolar system.

To exclude the possibility that improper vacuole acidification could have been the primary reason for the observed lack of α-factor degradation rather than an endocytic delivery defect, pheromone degradation was analyzed in *vat2* mutants disrupted for a subunit of the vacuolar ATPase. These cells display similar defects in vacuole acidification than *YPT51*-disrupted mutants. Interestingly, in spite of a delay in α-factor degradation to a $t_{1/2}$ of 16 min in *vat2* cells (data not shown) as compared with wild-type cells (10 min), this delay was much less severe than observed for *ypt51*, and especially for *ypt51ypt53*, *ypt51ypt52*, and *ypt51ypt52ypt53* mutants (see above). It is therefore highly unlikely that the lack of α-factor degradation in the here described *ypt* mutants was mainly caused by a lack of acidification.

Vesicle Accumulation and Vacuolar Morphology in ypt51, ypt52, and ypt53 Mutants

As Ypt51p, Ypt52p, and Ypt53p are likely to act in the endocytic and vacuolar protein sorting pathways, a morphological investigation by electron microscopy of *ypt51* and *ypt51-ypt52ypt53* mutants as compared to wild-type cells was initiated. Potassium permanganate fixation and staining was chosen, as it allows visualization of membrane structures without the need to remove the cell wall. It was observed that the *ypt51* null mutant (Fig. 8, *B* and *D*) as well as the triple

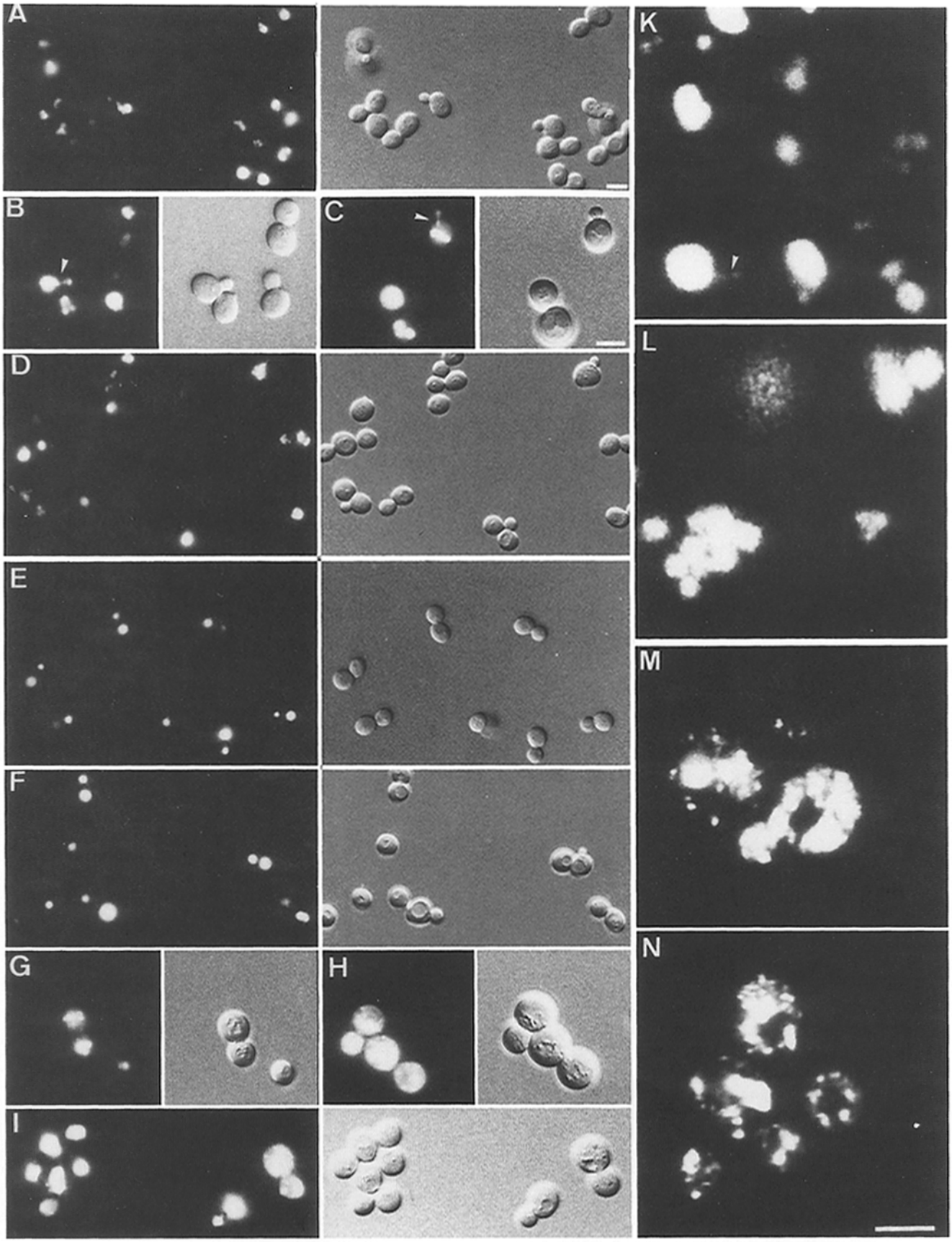
A
B
C
D
E
F
G
H
I
K
L
M
N

ypt51ypt52ypt53 mutant (Fig. 8 *C* and *E*) accumulated small vesicular structures with a diameter of ~40–60 nm. Compared with wild-type (Fig. 8 *A*), cells of both mutant strains contained on average 6–7-fold more of these vesicles. With respect to size, these structures resembled the vesicles accumulating in yeast mutants that are blocked in transport between the ER and the Golgi (Kaiser and Schekman, 1989; Becker et al., 1991). As we did not find any evidence for an impairment of CPY transport to the Golgi or for inhibition of protein secretion in Ypt51p-depleted cells, these accumulating type of vesicles are likely to represent transport intermediates between organelles other than the ER and the Golgi, perhaps endosomes.

Besides these morphological changes, thin section EM analysis did not reveal any other gross morphological changes, for example of the vacuolar system. However, due to the changed acidification properties and the appearance of small structures positive for LY in some of the *ypt* mutants, we also analyzed the vacuolar morphology on a larger cell population by light microscopy, using the vital stain carboxydichlorofluorescein diacetate (CDCFDA). Vacuolar labeling presumably results from diffusional uptake and subsequent hydrolysis of the dye by non-specific esterases, generating a fluorescent hydrolysis product (Pringle et al., 1989). In contrast to the microscopic analysis performed with LY, in which the cells were treated with energy poisons to stop endocytosis at a certain stage, these experiments were performed with metabolically active cells. Under these "optimal" conditions, typical vacuoles appear as multiple irregularly shaped organelles clustered in a certain region of the cell (Conradt et al., 1992) (Fig. 9, *A*, *B*, *K*, and *L*). During certain stages of the cell cycle a process termed vacuole inheritance induces the formation of so-called vacuolar segregation structures, which are projections formed by mother cell vacuoles leading into the developing bud (Weisman et al., 1987) (Fig. 9, *B*, *C*, and *K*, *arrowheads*).

Typical vacuoles and vacuolar segregation structures (*arrowheads*), as found in wild-type cells, were also observed in *ypt52*, *ypt53* (not shown), and *ypt52ypt53* null mutants (Fig. 9, *C* and *D*). In contrast to the convoluted vacuolar shapes of wild-type cells, vacuoles of *ypt51* mutants appeared completely spherical and as single structures (Fig. 9 *E*). Furthermore, the typical "tracks" formed by vacuolar material leading into the developing bud were never observed in these mutants, although larger buds clearly contained vacuoles. The spherical type of vacuole was also predominantly found in *ypt52ypt53* mutants (Fig. 9 *F*). However, numerous unusually small and bright structures were occasionally observed in these cells (Fig. 9 *G*). This type of staining became more frequent in *ypt51ypt52* and *ypt51ypt52ypt53* mutants (Fig. 9, *H* and *I*). Analysis of these cells by Nomarski optics revealed that the typical larger vacuolar organelles were replaced by much smaller structures. Confocal microscopy further resolved these brightly fluorescent entities into structures that seemed partly interconnected to form a CDCFDA-positive network (Fig. 9, *M* and *N*).

In summary, while EM analysis revealed the accumulation of small vesicular structures in thin sections of *ypt51* and *ypt51ypt52ypt53* mutants, subtle and differential morphological alterations of the vacuolar system could be observed in a small subset of the various *ypt* mutants with the help of a vital stain and light microscopy, which enables analysis of a large fraction of cells.

Discussion

Structural and Functional Similarities between Ypt51p, Ypt52p, and Ypt53p and Mammalian rab5 Proteins

In the present study three new members of the Ypt/rab family, Ypt51p, Ypt52p, and Ypt53p, were identified in *S. cerevisiae*, that share a high degree of identity/homology to rab5. Three criteria suggest that these small GTPases are structural homologs of rab5. First, a significant identity exists between the sequences of each of these Ypt protein and rab5 (48–54%). The identity is not as high as that between Yptlp and rablA (71%) (Haubruck et al., 1987), or Ypt7p and rab7 (63%) (Wichmann et al., 1992). On the other hand, rab8, which is required for transport from the TGN to the plasma membrane (Huber et al., 1993), thus providing evidence for functional similarity to Sec4p, is the closest structural homolog of Sec4p with 51% identity (Chavrier et al., 1992). Second, some of the structural elements that confer functional specificity to rab/Ypt proteins (located in the α2-helix [LAPMYYR] and effector domain [Stouten et al., 1993]) (Brennwald and Novick, 1993; Dunn et al., 1993; Haubruck et al., 1989; Hengst et al., 1990; Stenmark et al., 1994) are highly conserved between rab5 and Ypt51p, Ypt52p, and Ypt53p. Third, the phylogenetic analysis, which reflects the sum of similarities of individual sequence elements, clearly indicates that the rab5 proteins and the proposed *S. pombe* and *S. cerevisiae* homologs constitute a subgroup among all known small GTPases of the Ypt/rab family.

In addition to protein similarity, our data support the notion that, similar to rab5, the here described Ypt proteins are involved in the regulation of transport in the endocytic pathway. A strong inhibition of LY accumulation in the vacuole was observed for the single *Δypt51* mutant, which was further aggravated by the additional deletion of *YPT52* and *YPT53*. Furthermore, although *ypt51*, *ypt51ypt52* and *ypt51ypt52ypt53* null mutants displayed normal α-factor internalization rates, they were strongly impaired in α-factor degradation. As this process occurs in the vacuole, also this phenotype could be explained by an endocytic transport defect. This hypothesis is supported by the finding that, so far,

Figure 9. Vacuole morphology of various *ypt* mutants as compared with wild-type cells using CDCFDA as a vital stain. Wild-type and mutant cells were grown at 24°C to early logarithmic phase and resuspended in SD medium containing 50 mM citric acid, pH 5, and CDCFDA. After 20 min of staining at 30°C the cells were immediately viewed on concanavalin A-coated coverslips using a conventional fluorescence microscope equipped with Nomarski and fluorescence optics (*A–I*). Due to the increased fluorescence associated with *ypt51ypt52* and *ypt51ypt52ypt53* mutants the exposure time for micrographs was reduced sixfold as compared with the micrographs showing all other strains. Confocal fluorescence microscopy was used to analyze wild-type (*K* and *L*) and *ypt51ypt52ypt53* (*M* and *N*) cells. *A*, *B*, *K*, and *L*, wild-type cells; *C*, *D*, *ypt52ypt53*; *E*, *ypt51*; *F* and *G*, *ypt51ypt53*; *H*, *ypt51ypt52*; *I*, *M*, and *N*, *ypt51ypt52ypt53* mutants. Vacuolar segregation structures are indicated by arrowheads. Bars, 5 μm.

endocytic mutants (with recognizable vacuole) have all been shown to be defective in transport of both LY and α-factor (Kübler and Riezman, 1993; Raths et al., 1993). However, the surprising finding that *Δypt51* mutants displayed a dramatic reduction in the intracellular levels of mCPY under steady state conditions might suggest that inhibition of pheromone degradation could also be the result of a defect in vacuolar protease activity. While we cannot completely rule out this possibility, we think it is unlikely. The observation that proteinase A-dependent maturation of CPY and ALP is affected but does take place (even in *ypt51ypt52* and *ypt51-ypt52ypt53* mutants) suggests that the processing and degradative potential of the various *ypt* mutants is not severely impaired. Therefore, since pheromone degradation also depends on proteinase A (Singer and Riezman, 1990), it should take place if α-factor were present in the vacuole. Thus, we favor the idea that the lack of α-factor degradation in the here described *ypt* mutants is due to impaired transport to the site of degradation.

In conclusion, these data suggest that Ypt51p, Ypt52p, and Ypt53p are structurally and functionally related to rab5, although, without complementation analysis, we cannot definitively state at the present time that they correspond to the yeast counterparts of rab5A, B, and C.

Multiple Phenotypes of ypt51, ypt52, and ypt53 Mutants Suggest an Intersection of the Endocytic and Vacuolar Protein Sorting Pathways

Besides the defect in the delivery of endocytic markers to the vacuole, the various *ypt* mutants displayed phenotypes that are reminiscent of *vps* mutants (Raymond et al., 1992). These include a delay in the maturation of vacuolar hydrolases, partial missorting of the Golgi form of vacuolar CPY to the extracellular space, acidification defects and subtle morphological alterations of the vacuolar system. In fact, *vps21* (Robinson et al., 1988) represents a mutant allele of *YPT51* (Emr, S., personal communication).

In light of the multiple phenotypes displayed by the here described *ypt* mutants, the question could be raised whether the defect in acidification may be responsible for the missorting of p2CPY and the inhibition of α-factor degradation. Previous studies have revealed that lack of vacuolar acidification has severe implications on intracellular transport pathways. Treatment of cells with bafilomycin A1, a specific inhibitor of the vacuolar ATPase, results in missorting of CPY (Banta et al., 1988) to the same extent as observed for the *Δypt51* mutants. However, neither missorting of ALP (Klionsky and Emr, 1989) nor a major defect in α-factor degradation occurs (Singer and Riezman, 1990). In mutants disrupted for a gene encoding a subunit of the vacuolar ATPase (*vat2* or *vatB*) the extent of missorting of CPY to the extracellular medium was similar to that of bafilomycin A1-treated cells, while maturation of p2CPY to mCPY was further delayed and precursor ALP accumulated (Klionsky et al., 1992). Nevertheless, even if α-factor degradation was delayed in *vat2* cells, its $t_{1/2}$ was only 16 min, whereas in Ypt51p-depleted cells it was prolonged to 48 min. Therefore, while it is possible that the acidification defect in the here described *ypt* mutants leads to missorting and precursor accumulation of vacuolar enzymes, it seems unlikely that it could be the primary reason for lack of α-factor degradation.

It rather seems that the phenotypes displayed by *ypt51*, *ypt52*, and *ypt53* mutants could well be explained by a transport defect affecting an endocytic organelle which is connected with the vacuolar sorting pathway. Experimental evidence for the meeting of the two pathways comes from cell-fractionation analysis, which reveals that p2CPY and endocytosed α-factor cofractionate in a prevacuolar/endosomal compartment (Vida et al., 1993). Independently, studies with the *ypt7* null mutant have suggested that meeting of endocytosed α-factor with vacuolar hydrolases might occur before delivery to the vacuole, since a *PEP4*-dependent and energy-independent pheromone degradation can be observed in this mutant (Schimmöller and Riezman, 1993). Finally, the finding that Renlp, a protein identified for its role in the delivery of α-factor receptor to the vacuole, is identical to Vps2p (Davis et al., 1993), which is required for vacuolar protein sorting, also provides further evidence for the intersection of the endocytic with the vacuolar protein sorting pathway.

Site of Function of Ypt5 Proteins

Due to the complexity of the *ypt51-*, *ypt52-*, and *ypt53*-associated phenotypes, it is too early to pinpoint the precise step controlled by these Ypt proteins. However, phenotypic comparison between *Δypt7* and the here described *ypt* mutants provides some clues about the order in which these small GTPases might function. Ypt7p, the yeast homolog of mammalian rab7 which is associated with late endosomes (Chavrier et al., 1990), has been suggested by Wichmann et al. (1992) to play a role in the endocytic transport of α-factor to the vacuole. As in the here described *ypt* mutants, indirect evidence for this was a substantial delay of endocytosed pheromone degradation in a *Δypt7* mutant. A number of observations support the idea that Ypt51p, Ypt52p, and Ypt53p proteins may act at an earlier step in the endocytic pathway than Ypt7p. First, by comparing the patterns of degradation in *ypt7* and *ypt51*, *ypt52*, and *ypt53* mutants obtained under the same experimental conditions, it becomes clear that α-factor degradation is more severely inhibited in the latter mutants. Second, vacuole fragmentation can be predominantly observed in *Δypt7* mutants, but is only occasionally seen in the here described *ypt* mutants. Third, since in yeast at least two kinetic endosomal intermediates (early and late endosomes) can be distinguished (Singer and Riezman, 1990; Singer-Krüger et al., 1993), it is interesting to note that recent studies on the *ypt7* null mutant have revealed an accumulation of endocytosed α-factor in a gradient fraction enriched for late endosomes (Schimmöller and Riezman, 1993). This suggests that Ypt7p is required for transport from late endosomes to the vacuole (Schimmöller and Riezman, 1993). Conversely, preliminary cell fractionation experiments suggest that upon internalization of α-factor into the *ypt51* null mutant, the pheromone accumulates in a prevacuolar endocytic compartment, most likely in early endosomes as defined by Singer-Krüger et al. (1993) (Singer-Krüger, B., and M. Zerial, unpublished observations). The proposed order of function of Ypt51p and Ypt7p would be in accordance with the proposed successive function of mammalian rab5 and rab7. Future experiments, like epistasis analysis with *ypt51ypt7* double mutants, will hopefully help to test this working hypothesis.

While the internalization rate of transferrin can be modulated by rab5 in mammalian cells (Bucci et al., 1992), it is at present still unclear why the deletion of *YPT51*, *YPT52*, and *YPT53* does not affect the internalization rate of α-factor in yeast.

Morphological Changes in ypt51, ypt52, and ypt53 Mutants

Analysis of the vacuolar morphology of the various *ypt* mutants using CDCFDA staining in living cells and light microscopy revealed that the *ypt51* mutant contained a single large vacuole, which was completely spherical, in contrast to the convoluted vacuolar structures observed in wild-type cells. In addition, vacuolar segregation structures were not found in *ypt51* mutants. The single, spherical type of vacuole was also found predominately in the *ypt51ypt52*, *ypt51ypt53*, and *ypt51ypt52ypt53* mutants. However, in the latter mutants, a small but significant number of cells displayed fragmented vacuolar structures. The observation that these structures were also labeled with LY would favor an endosomal origin. Simultaneous disappearance of typical vacuolar elements in these particular cells would then support the idea that vacuole biogenesis depends on proper endocytic and vacuolar protein transport, as discussed before.

Furthermore, the 40–60-nm vesicles which accumulate in *ypt51* and *ypt51ypt52ypt53* mutants, revealed by EM analysis, may correspond to transport intermediates of the endocytic and/or vacuolar protein sorting pathways. Their resemblance in size to vesicles accumulating in mutants that are blocked in transport between the ER and the Golgi might be rather coincidental, since no such transport defect could be observed in the here described *ypt* mutants. Definite proof for the origin of these vesicular structures will await more detailed ultrastructural and cell fractionation analysis. The finding that morphological changes of the vacuolar system were not observed by EM, most likely can be explained by the fact that first, these changes might be only visible in living cells, and second, that they are only apparent upon analysis of a large number of cells.

Functional Redundance of Ypt51p, Ypt52p, and Ypt53p?

The existence of three similar Ypt proteins raises the question whether they might be functionally redundant or play specialized and distinct roles. Since in all respects the most severe defects were associated with the *ypt51* mutant compared to the other two single mutants, it seems that Ypt51p is the most essential protein for the general endocytic pathway. On the other hand, detectable aggravation of all analyzed phenotypes (growth, endocytosis, vacuolar protein missorting, acidification, vacuolar morphology) upon additional disruption of *YPT52* and *YPT53* demonstrates that the three gene products have at least overlapping functions. The role of Ypt53p in endocytic traffic (or any other transport step) is more elusive than that for Ypt51p and Ypt52p. Its involvement in these transport pathways is, however, suggested in double *ypt51ypt53*, *ypt52ypt53* and the triple *ypt51ypt52ypt53* mutants, in which synergistic effects can be observed. Nevertheless, the sole presence of Ypt53p in *ypt51ypt52* mutants does not complement the absence of the other two small GTPases, as no major phenotypic differences to the triple mutant could be detected. Therefore, it is possible that Ypt53p may have a very specialized, yet unresolved function. Interestingly, the severity of the mutant phenotypes correlates well with the predicted abundance of the respective proteins: Ypt51p and Ypt52p, which seem to be more important for the general endocytic pathway, have a higher value of theoretical protein abundance, whereas the low abundance calculated for Ypt53p would be in agreement with a specialized and less general function.

We are indebted to Hans-Heinrich Trepte for performing the electron microscopic analyses. We would like to thank Tim Stearns for generously sharing unpublished information and providing a PCR fragment containing a partial sequence of *YPT53*, Scott Emr for kindly sharing unpublished sequence information on *VPS21*, and Michael Hall for generously providing the yeast genomic library. We are grateful to Alfonso Valencia for the phylogenetic analysis and Angelika Giner for excellent technical assistance. We gratefully acknowledge Bernard Hoflack, Rob Parton, and Howard Riezman for critical reading of the manuscript.

This research was supported by grants from the Deutsche Forschungsgemeinschaft (to D. Gallwitz), the Human Frontier Science Program (to M. Zerial and D. Gallwitz) and the BRIDGE program of the European Community (to P. Philippsen). B. Singer-Krüger is a recipient of a postdoctoral long-term EMBO fellowship, H. Stenmark of a postdoctoral fellowship from the Research Council of Norway.

Received for publication 20 August 1993, and in revised form 12 January 1994.

References

Achstetter, T., A. Franzusoff, C. Field, and R. Schekman. 1988. *SEC7* encodes an unusual, high molecular weight protein required for membrane traffic from the yeast Golgi apparatus. *J. Biol. Chem.* 263:11711–11717.

Adari, H., D. R. Lowy, B. M. Willumsen, C. J. Der, and F. McCormick. 1988. Guanosine triphosphatase activating protein (GAP) interacts with the p21 *ras* effector binding domain. *Science (Wash. DC).* 240:518–521.

Armstrong, J., M. W. Craighead, R. Watson, S. Ponnambalam, and S. Bowden. 1993. *Schizosaccharomyces pombe* ypt5: A homologue of the rab5 endosome fusion regulator. *Mol. Biol. Cell.* 4:583–592.

Banta, L. M., J. S. Robinson, D. J. Klionsky, and S. D. Emr. 1988. Organelle assembly in Yeast: Characterization of yeast mutants defective in vacuolar biogenesis and protein sorting. *J. Cell Biol.* 107:1369–1383.

Becker, J., T. J. Tan, H.-H. Trepte, and D. Gallwitz. 1991. Mutational analysis of the putative effector domain of the GTP-binding Ypt1 protein in yeast suggests specific regulation by a novel GAP activity. *EMBO (Eur. Mol. Biol. Organ.) J.* 10:785–792.

Bennetzen, J. L., and B. D. Hall. 1982. Codon selection in yeast. *J. Biol. Chem.* 257:3026–3031.

Brennwald, P., and P. Novick. 1993. Interactions of three domains distinguishing the Ras-related GTP-binding proteins Ypt1 and Sec4. *Nature (Lond.).* 362:560–563.

Bucci, C., R. G. Parton, I. H. Mather, H. Stunnenberg, K. Simons, B. Hoflack, and M. Zerial. 1992. The small GTPase rab5 functions as a regulatory factor in the early endocytic pathway. *Cell.* 70:715–728.

Cales, C., J. F. Hancock, C. F. Marshall, and A. Hall. 1988. The cytoplasmic protein GAP is implicated as the target for regulation by the *ras* gene product. *Nature (Lond.).* 332:548–551.

Chavrier, P., R. G. Parton, H.-P. Hauri, K. Simons, and M. Zerial. 1990. Localization of low molecular weight GTP binding proteins to exocytic and endocytic compartments. *Cell.* 62:317–329.

Chavrier, P., K. Simons, and M. Zerial. 1992. The complexity of the Rab and Rho GTP-binding protein subfamilies revealed by a PCR cloning approach. *Gene (Amst.).* 112:261–264.

Conradt, B., J. Shaw, T. Vida, S. Emr, and W. Wickner. 1992. In vitro reactions of vacuolar inheritance in *Saccharomyces cerevisiae*. *J. Cell Biol.* 119:1469–1479.

Davis, N. G., Horecka, J. L., and G. F. Sprague, Jr. 1993. *Cis-* and *Trans*-acting functions required for endocytosis of the yeast pheromone receptors. *J. Cell Biol.* 122:53–65.

Dulic, V., M. Egerton, I. Elguindi, S. Raths, B. Singer, and H. Riezman. 1991. Yeast endocytosis assays. *Methods Enzymol.* 194:679–710.

Dunn, B., T. Stearns, and D. Botstein. 1993. Specificity domains distinguish the Ras-related GTPases Ypt1 and Sec4. *Nature (Lond.).* 362:563–565.

Emr, S. D., A. Vassarotti, J. Garrett, B. L. Geller, M. Takeda, and M. G. Douglas. 1986. The amino terminus of the yeast F1-ATPase β-subunit

precursor functions as a mitochondrial import signal. *J. Cell Biol.* 102: 523–533.
Gorvel, J.-P., P. Chavrier, M. Zerial, and J. Gruenberg. 1991. Rab5 controls early endosome fusion in vitro. *Cell.* 64:915–925.
Haubruck, H., C. Disela, P. Wagener, and D. Gallwitz. 1987. The *ras*-related *ypt* protein is a ubiquitous eukaryotic protein: isolation and sequence analysis of mouse cDNA clones highly homologous to the yeast *YPT1* gene. *EMBO (Eur. Mol. Biol. Organ.) J.* 6:4049–4053.
Haubruck, H., R. Prange, C. Vorgias, and D. Gallwitz. 1989. The *ras*-related mouse ypt1 protein can functionally replace the *YPT1* gene product in yeast. *EMBO (Eur. Mol. Biol. Organ.) J.* 8:1427–1432.
Heitman, J., N. R. Movva, P. Hiestand, and M. N. Hall. 1991. FK 506-binding protein proline rotamase is a target for the immunosuppressive agent FK 506 in *Saccharomyces cerevisiae. Proc. Natl. Acad. Sci. USA.* 88:1948–1952.
Hengst, L., T. Lehmeier, and D. Gallwitz. 1990. The *rhy1* gene in the fission yeast *Schizosaccharomyces pombe* encoding a GTP-binding protein related to ras, rho and ypt: structure, expression and identification of its human homologue. *EMBO (Eur. Mol. Biol. Organ.) J.* 9:1949–1955.
Higgins, D. G., A. J. Bleasby, and R. Fuchs. 1992. CLUSTAL V: improved software for multiple sequence alignment. *Comput. Appl. Biosci.* 8:189–191.
Huber, L. A., S. Pimplikar, R. G. Parton, H. Virta, M. Zerial, and K. Simons. 1993. Rab8, a small GTPase involved in vesicular traffic between the TGN and the basolateral plasma membrane. *J. Cell Biol.* 123:35–45.
Kaiser, C. A., and R. Schekman. 1989. Distinct sets of *SEC* genes govern transport vesicle formation and fusion early in the secretory pathway. *Cell.* 61:723–733.
Klionsky, D. J., and S. D. Emr. 1989. Membrane protein sorting: biosynthesis, transport and processing of yeast vacuolar alkaline phosphatase. *EMBO (Eur. Mol. Biol. Organ.) J.* 8:2241–2250.
Klionsky, D. J., H. Nelson, and N. Nelson. 1992. Compartment acidification is required for efficient sorting of proteins to the vacuole in *Saccharomyces cerevisiae. J. Biol. Chem.* 267:3416–3422.
Kübler, E., and H. Riezman. 1993. Actin and fimbrin are required for the internalization step of endocytosis in yeast. *EMBO (Eur. Mol. Biol. Organ.) J.* 12:2855–2862.
Lombardi, D., T. Soldati, M. A. Riederer, Y. Goda, M. Zerial, and S. Pfeffer. 1993. rab9 functions in transport between late endosomes and the trans Golgi network. *EMBO (Eur. Mol. Biol. Organ.) J.* 12:677–682.
Nelson, H., and N. Nelson. 1990. Disruption of genes encoding subunits of yeast vacuolar H^+-ATPase causes conditional lethality. *Proc. Natl. Acad. Sci. USA.* 87:3503–3507.
Orr-Weaver, T., J. Szostak, and R. Rothstein. 1981. Yeast transformation: a model system to study of recombination. *Proc. Natl. Acad. Sci. USA.* 78:6354–6358.
Ossig, R., Dascher, C., Trepte, H.-H., Schmitt, H. D., and D. Gallwitz. 1991. The yeast *SLY* gene products, suppressors of defects in the essential GTP-binding Ypt1 protein, may act in endoplasmic reticulum-to-Golgi transport. *Mol. Cell Biol.* 11:2980–2993.
Payne, G. S., D. Baker, E. van Tuinen, and R. Schekman. 1988. Protein transport to the vacuole and receptor-mediated endocytosis by clathrin heavy chain-deficient yeast. *J. Cell Biol.* 106:1453–1461.
Philippsen, P., A. Stotz, and C. Scherf. 1991. DNA of *Saccharomyces cerevisiae. Methods Enzymol.* 194:169–182.
Preston, R. A., R. F. Murphy, and E. W. Jones. 1989. Assay of vacuolar pH in yeast and identification of acidification-defective mutants. *Proc. Natl. Acad. Sci. USA.* 1989:7027–7031.
Pringle, J. R., R. A. Preston, A. E. M. Adams, T. Stearns, D. G. Drubin, B. K. Haarer, and E. W. Jones. 1989. Fluorescence microscopy methods for yeast. *Methods Cell Biol.* 31:357–435.
Raths, S., J. Rohrer, F. Crausaz, and H. Riezman. 1993. *end3* and *end4*: two mutants defective in receptor-mediated and fluid-phase endocytosis in *Saccharomyces cerevisiae. J. Cell Biol.* 120:55–65.
Raymond, C. K., I. Howald-Stevenson, C. A. Vater, and T. H. Stevens. 1992. Morphological classification of the yeast vacuolar protein sorting mutants: evidence for a prevacuolar compartment in class E *vps* mutants. *Mol. Biol. Cell.* 3:1389–1402.
Riezman, H. 1993. Yeast endocytosis. *Trends Cell Biol.* 3:273–277.
Roberts, C. J., C. K. Raymond, C. T. Yamashiro, and T. H. Stevens. 1991. Methods for studying the yeast vacuole. *Methods Enzymol.* 194:644–661.
Robinson, J. S., D. J. Klionsky, L. M. Banta, and S. D. Emr. 1988. Protein sorting in *Saccharomyces cerevisiae*: isolation of mutants defective in the delivery and processing of multiple vacuolar hydrolases. *Mol. Cell. Biol.* 8:4936–4948.
Rothman, J. H., I. Howald, and T. H. Stevens. 1989*a*. Characterization of genes required for protein sorting, vacuolar function, and endocytosis in the yeast *Saccharomyces cerevisiae. EMBO (Eur. Mol. Biol. Organ.) J.* 8:2057–2065.
Rothman, J. H., C. T. Yamashiro, C. K. Raymond, P. M. Kane, and T. H. Stevens. 1989*b*. Acidification of the lysosome-like vacuole and the vacuolar H^+-ATPase are deficient in two yeast mutants that fail to sort vacuolar proteins. *J. Cell Biol.* 109:93–100.
Salminen, A., and P. Novick. 1987. A ras-like protein is required for a post-Golgi event in yeast secretion. *Cell.* 49:527–538.
Sambrook, J., M. E. Frisch, and T. Maniatis. 1989. Molecular cloning: a laboratory manual, 2nd edition. Cold Spring Harbor Laboratory Press, Cold Spring Harbor, NY.
Schimmöller, F., and H. Riezman. 1993. Involvement of Ypt7p, a small GTP-binding protein, in traffic from late endosome to the vacuole in yeast. *J. Cell Sci.* 106:823–830.
Schmitt, H. D., M. Puzicha, and D. Gallwitz. 1988. Study of a temperature-sensitive mutant of the *ras*-related YPT1 gene product in yeast suggests a role in the regulation of intracellular calcium. *Cell.* 53:635–647.
Segev, N., J. Mulholland, and D. Botstein. 1988. The yeast GTP-binding YPT1 protein and a mammalian counterpart are associated with the secretion machinery. *Cell.* 52:915–924.
Simons, K., and M. Zerial. 1993. Rab proteins and the road maps for intracellular transport. *Neuron.* 11:789–799.
Singer, B., and H. Riezman. 1990. Detection of an intermediate compartment involved in transport of α-factor from the plasma membrane to the vacuole in yeast. *J. Cell Biol.* 110:1911–1922.
Singer-Krüger, B., R. Frank, F. Crausaz, and H. Riezman. 1993. Partial purification and characterization of early and late endosomes from yeast. *J. Biol. Chem.* 268:14376–14386.
Stenmark, H., A. Valencia, O. Martinez, O. Ullrich, B. Goud, and M. Zerial. 1994. Distinct structural elements define the junctional specificity of rab5. *EMBO (Eur. Mol. Biol. Organ.) J.* 13:575–583.
Stevens, T., B. Esmon, and R. Schekman. 1982. Early stages in the yeast secretory pathway are required for transport of carboxypeptidase Y to the vacuole. *Cell.* 30:439–448.
Stouten, P. F., C. Sander, A. Wittinghofer, and A. Valencia. 1993. How does the switch II region of G-domains work? *FEBS (Fed. Eur. Biochem. Soc.) Lett.* 320:1–6.
Touchot, N., P. Chardin, and A. Tavitian. 1987. Four additional members of the *ras* gene superfamily isolated by an oligonucleotide strategy: molecular cloning of YPT related cDNAs from a rat brain library. *Proc. Natl. Acad. Sci. USA.* 84:8210–8214.
Towbin, H., T. Staehelin, and J. Gordon. 1979. Electrophoretic transfer of proteins from polyacrylamide gels to nitrocellulose sheets: procedure and some applications. *Proc. Natl. Acad. Sci. USA.* 76:4350–4354.
Valencia, A., P. Chardin, A. Wittinghofer, and C. Sander. 1991. The *ras* protein family: Evolutionary tree and role of conserved amino acids. *Biochemistry.* 30:4637–4648.
van der Sluijs, P., M. Hull, A. Zahraoui, A. Tavitian, B. Goud, and I. Mellman. 1991. The small GTP-binding protein rab4 is associated with early endosomes. *Proc. Natl. Acad. Sci. USA.* 88:6313–6317.
van der Sluijs, P., M. Hull, P. Webster, P. Male, B. Goud, and I. Mellman. 1992. The small GTP-binding protein rab4 controls an early sorting event on the endocytic pathway. *Cell.* 70:729–740.
Vida, T. A., G. Huyer, and S. D. Emr. 1993. Yeast vacuolar proenzymes are sorted in the late Golgi complex and transported to the vacuole via a prevacuolar endosome-like compartment. *J. Cell Biol.* 121:1245–1256.
Weisman, L. S., R. Bacallao, and W. Wickner. 1987. Multiple methods of visualizing the yeast vacuole permit evaluation of its morphology and inheritance during the cell cycle. *J. Cell Biol.* 105:1539–1547.
Wichmann, H., L. Hengst, and D. Gallwitz. 1992. Endocytosis in yeast: evidence for the involvement of a small GTP-binding protein (Ypt7p). *Cell.* 71:1131–1142.
Winship, P. R. 1989. An improved method for directly sequencing PCR amplified material using dimethyl sulfoxide. *Nucleic Acids Res.* 17:1266.
Yamashiro, C. T., P. M. Kane, D. F. Wolczyk, R. A. Preston, and T. H. Stevens. 1990. Role of vacuolar acidification in protein sorting and zymogen activation: a genetic analysis of the yeast vacuolar proton-translocating ATPase. *Mol. Cell. Biol.* 10:3737–3749.
Zahraoui, A., N. Touchot, P. Chardin, and A. Tavitian. 1989. The human rab genes encode a family of GTP-binding proteins related to yeast YPT1 and SEC4 products involved in secretion. *J. Biol. Chem.* 164:12394–12401.
Zerial, M., and H. Stenmark. 1993. Rab GTPases in vesicular transport. *Curr. Opin. Cell Biol.* 5:613–620.